Managing for ecological surprises in metapopulations

2	Supplemental materials: Model details & results
3	Kyle L. Wilson ^a , Alex Sawyer ^a , Anna Potapova ^a , Colin J. Bailey ^a , Elissa Sweeney-Bergen ^a ,
4	Emma E. Hodgson ^a , Kara J. Pitman ^a , Karl Seitz ^a , Lauren Law ^a , Luke Warkentin ^a ,
5	Samantha M. Wilson ^a , William I. Atlas ^a , Daniella LoScerbo ^b , Douglas C. Braun ^c , Matthew
6	R. Sloat ^{d} , M. Tim Tinker ^{e} , and Jonathan W. Moore ^{a,b}
7	
8	^a Earth to Ocean Research Group, Simon Fraser University
9	^b Resource and Environmental Management, Simon Fraser University
0	^c Fisheries and Oceans Canada
1	d Wild Salmon Center
2	$^e\mathrm{Ecology}$ and Evolutionary Biology, University of California Santa Cruz
3	22 July 2019
	v

Contents

15	Metapopulation model
16	Local & metapopulation dynamics
17	Creating the spatial networks
18	Dispersal
19	Disturbance regimes
20	Recruitment stochasticity
21	Post-disturbance outcomes
22	Monitoring & management at aggregate-scale
23	Finding maximum sustainable yield
24	Scenarios
25	Example results
26	General patterns
27	Effects of disturbance regime
28	Role of network structure & dispersal
29	General patterns in MSY
30	General patterns in the risk of hysteresis & state shifts
31	General patterns in the risk of spatial contraction
32	References

^{*}Corresponding author - email: kl_wilson@sfu.ca

33 Metapopulation model

Local & metapopulation dynamics

- Our metapopulation is defined by a set of local populations N_p for a species with a one year generation time
- with time-dynamics that follows birth (i.e., recruitment R), immigration, death, and emigration (BIDE)
- processes typical to metapopulation theory (Hanski 1998):

$$N_{it+1} = R_{it}\epsilon_{it} + I_{it} - D_{it} - E_{it} \tag{1}$$

- where N_{it+1} is the number of adults in patch i at time t, R_{it} is number of recruits, I_{it} is number of recruits
- immigrating into patch i from any other patch, D_{it} is number of recruits that die due to disturbance regime,
- E_{it} is the number of recruits emigrating from patch i into any other patch, and E_{it} is stochasticity in
- 41 recruitment.
- Resoure monitoring often occurs at the scale of the metapopulation (Anderson et al. 2015), hence we define
- 43 metapopulation adults as:

$$MN_t = \sum_{i=1}^{N_p} N_{it} \tag{2}$$

with metapopulation recruits:

$$MR_t = \sum_{i=1}^{N_p} R_{it} \tag{3}$$

- 45 Local patch recruitment at time t depended on adult densities at t-1 and followed a reparameterized
- 46 Beverton-Holt function:

$$R_{it} = \frac{\alpha_i N_{it-1}}{1 + \frac{\alpha_i - 1}{\beta_i} N_{it-1}} \tag{4}$$

- where α_i is the recruitment compensation ratio and β_i is local patch carrying capacity.
- 48 Management often monitors metapopulation resources as the aggregate of all local populations. For example,
- take a two patch metapopulation model that varies α_i and β_i parameters where:

- Here, recruitment compensation from local patches α_i gets averaged across the metapopulation leading to an
- average compensation ratio $\bar{\alpha}$ of 3. Likewise, the total carrying capacity of the metapopulation $\bar{\beta}$ becomes
- the summation of local patch carrying capacities $\sum \beta_i$, which is 300. This scale of monitoring generates the
- following local patch and metapopulation dynamics:

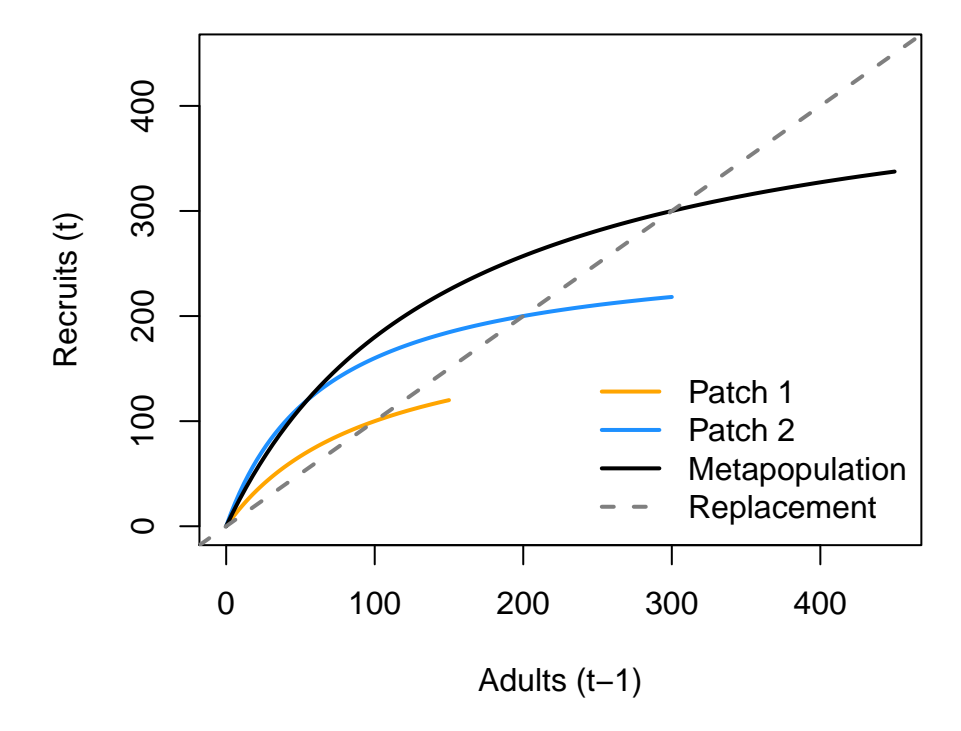


Figure S1: Metapopulation and local patch recruitment dynamics.

54 Creating the spatial networks

- The next aspect to our metapopulation model is connecting the set of patches to one another (Yeakel et al.
- ⁵⁶ 2014). We need to specify the number of patches, their arrangements (i.e., connections), and how far apart
- 57 they are from one another. We followed some classic metapopulation and source-sink arrangements to create
- four networks that generalize across a few real-world topologies: a linear habitat network (e.g., coastline), a
- 59 dendritic or branching network (e.g., coastal rivers), a star network (e.g., mountain & valley, or lake with
- 60 inlet tributaries), and a complex network (e.g., terrestrial plants).
- To make networks comparable, each spatial network type needs the same leading parameters (e.g., number of
- patches N_p and mean distance between neighboring patches \bar{d}). In this case, we set N_p to 16 and \bar{d} to 1 unit
- 63 (distance units are arbitrary). We used the igraph package (Csardi & Nepusz 2006) and some custom code
- to arrange our spatial networks as the following:

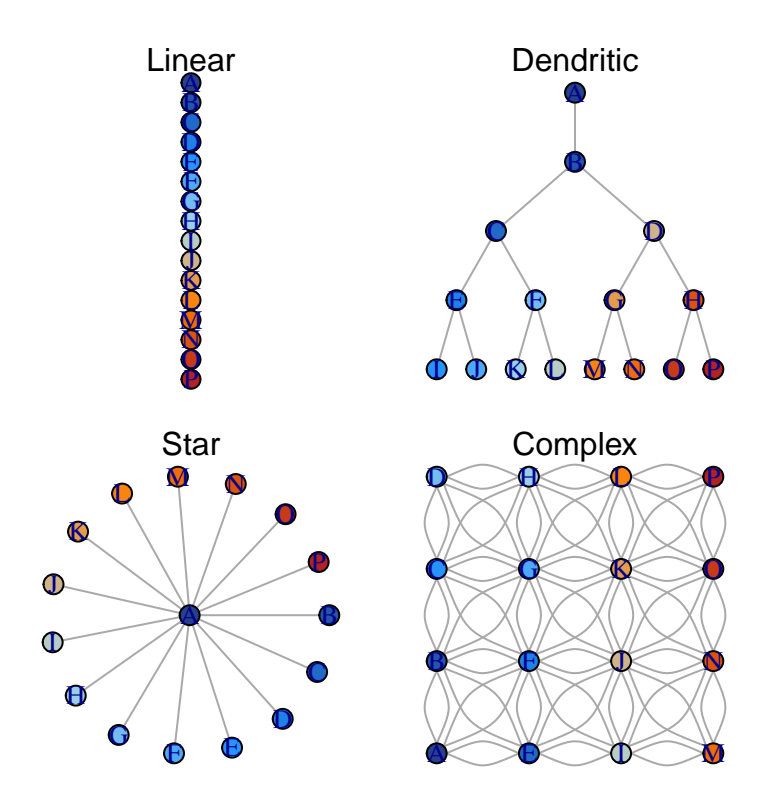


Figure S2: Four spatial network topologies.

Note that distances between neighbor patches in the above networks are equal.

66 An example dispersal matrix for the complex network:

```
ABEFCGDHIJKLMNOP
   ## A O 1 1 1 2 2 3 3 2 2 2 3 3 3 3 3
   ## B 1 0 1 1 1 1 2 2 2 2 2 2 3 3 3 3
69
   ## E 1 1 0 1 2 2 3 3 1 1 2 3 2 2 2 3
   ## F 1 1 1 0 1 1 2 2 1 1 1 2 2 2 2 2
71
   ## C 2 1 2 1 0 1 1 1 2 2 2 2 3 3 3 3
72
   ## G 2 1 2 1 1 0 1 1 2 1 1 1 2 2 2 2
73
   ## D 3 2 3 2 1 1 0 1 3 2 2 2 3 3 3 3
   ## H 3 2 3 2 1 1 1 0 3 2 1 1 3 2 2 2
75
   ## I 2 2 1 1 2 2 3 3 0 1 2 3 1 1 2 3
   ## J 2 2 1 1 2 1 2 2 1 0 1 2 1 1 1 2
77
   ## K 2 2 2 1 2 1 2 1 2 1 0 1 2 1 1 1
   ## L 3 2 3 2 2 1 2 1 3 2 1 0 3 2 1 1
79
   ## M 3 3 2 2 3 2 3 3 1 1 2 3 0 1 2 3
   ## N 3 3 2 2 3 2 3 2 1 1 1 2 1 0 1 2
   ## 0 3 3 2 2 3 2 3 2 2 1 1 1 2 1 0 1
   ## P 3 3 3 2 3 2 3 2 3 2 1 1 3 2 1 0
```

84 Dispersal

Dispersal from patch i into patch j depends on constant dispersal rate ω (defined as the proportion of total local recruits that will disperse) and an exponential distance-decay function between i and j with distance cost to dispersal m following Anderson et al. (2015):

$$E_{ij(t)} = \omega R_{it} p_{ij} \tag{5}$$

where E_{ij} is the total dispersing animals from patch i into patch j resulting from dispersal rate ω , total number of local recruits R_{it} , and probability of dispersal between patches p_{ij} :

$$p_{ij} = \frac{e^{-md_{ij}}}{\sum\limits_{\substack{j=1\\j\neq i}}^{N_p} e^{-md_{ij}}}$$

$$(6)$$

where d_{ij} is the pairwise distance between patches, m is the distance cost to dispersal. The summation term in the denominator normalizes the probability of moving to any patch to between 0 and 1 with the constraint that dispersers cannot move back into their home patch (i.e., $j \neq i$. With $\bar{d} = 1$, m = 0.5, $\omega = 0.1$, $R_{it} = 100$ in a linear network:

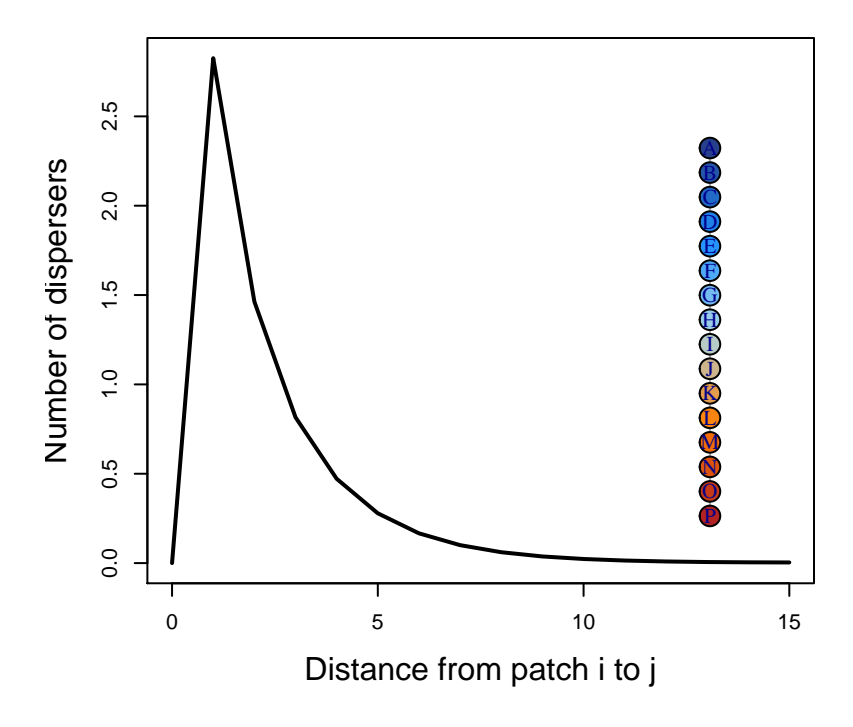


Figure S3: Example dispersal patterns across linear network.

94 Disturbance regimes

- In all scenarios, disturbance was applied after 50 years of equilibrating the metapopulaton at pristine
- conditions. At year 51, we applied the disturbance regime (the regime varied from uniform, localized,
- 97 random, and localized, extirpation see Scenarios below). Disturbance immediately removes a set proportion
- of the metapopulation adults at that time (i.e., 0.9 of $MN_{t=51}$). Once applied, the metapopulation was no
- 99 longer disturbed and spatio-temporal recovery dynamics emerged naturally from these new conditions.

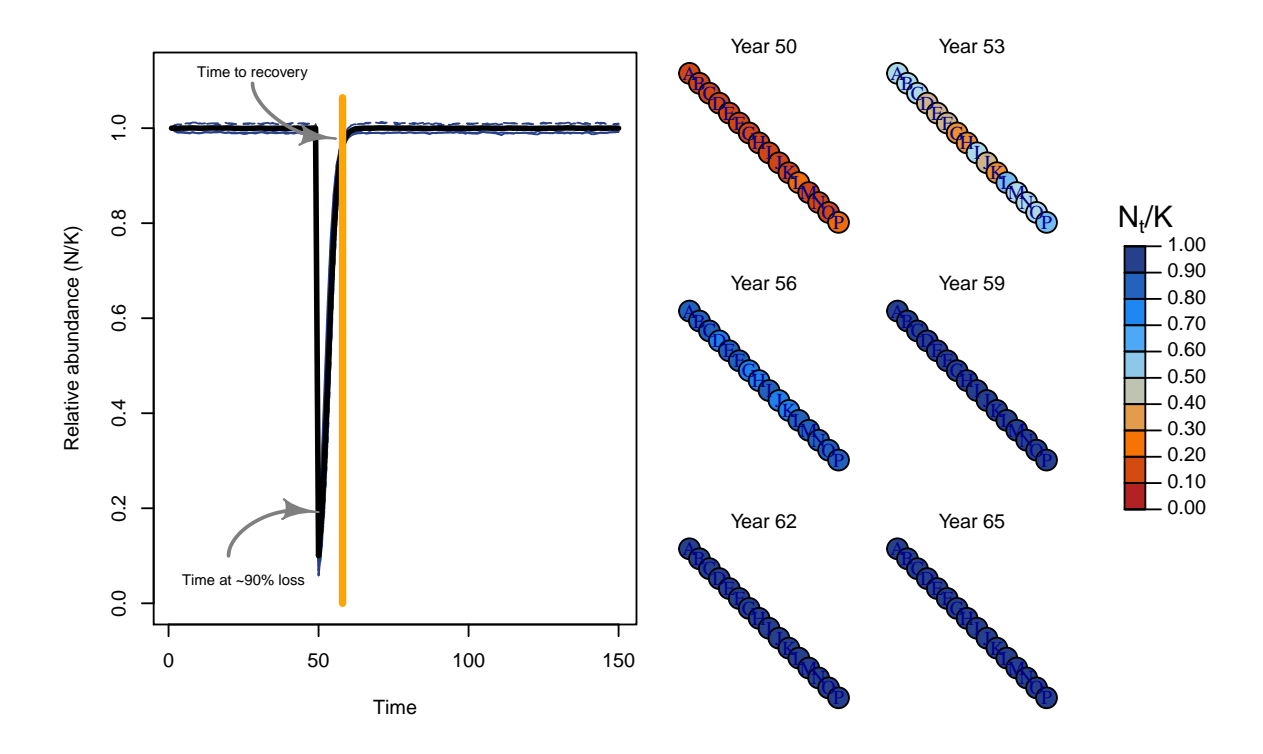


Figure S4: Recovery regime of metapopulation with linear topology through time (left) and space (right).

100 Recruitment stochasticity

Our model allowed for stochastic recruitment that followed a lognormal distribution with average variation in recruitment of σ_R . In cases of stochastic recruitment, the expected recruitment:

$$R_{it} = \frac{\alpha_i N_{it-1}}{1 + \frac{\alpha_i - 1}{\beta_i} N_{it-1}} \tag{7}$$

103 becomes:

104

105

106

107

108

$$R_{it} = \frac{\alpha_i N_{it-1}}{1 + \frac{\alpha_i - 1}{\beta_i} N_{it-1}} e^{(\epsilon_{it} - \frac{\ln(\sigma_R^2 + 1)}{2})}$$
(8)

where lognormal deviates for each patch i at time t are drawn from a multivariate normal distribution (MVN) If σ_R is low, then metapopulation dynamics approach the deterministic case. In some scenarios, we evaluate the role of spatially and/or temporally correlated deviates across the metapopulations to model potential common drivers affecting metapopulation dynamics (e.g., Moran effects). Expected recruitment deviates followed a first-order autoregression model such that:

$$\epsilon_{it} = \rho_T \epsilon_{t-1} + MVN(\mu = 0, \Sigma = \sigma_R (1 - \rho_T^2) e^{(-\rho_S D_{ij})})$$

$$\tag{9}$$

109

110

111

where ρ_T is temporal correlation (bounded 0-1) ρ_S is rate of distance-decay in spatial correlation (bounded $0-\infty$ with higher values leading to independent patches). If rho_T is 0 and rho_S is high, then annual recruitment deviates are independent. We illustrate the effects of four kinds of recruitment deviates below using the same random number generator seed:

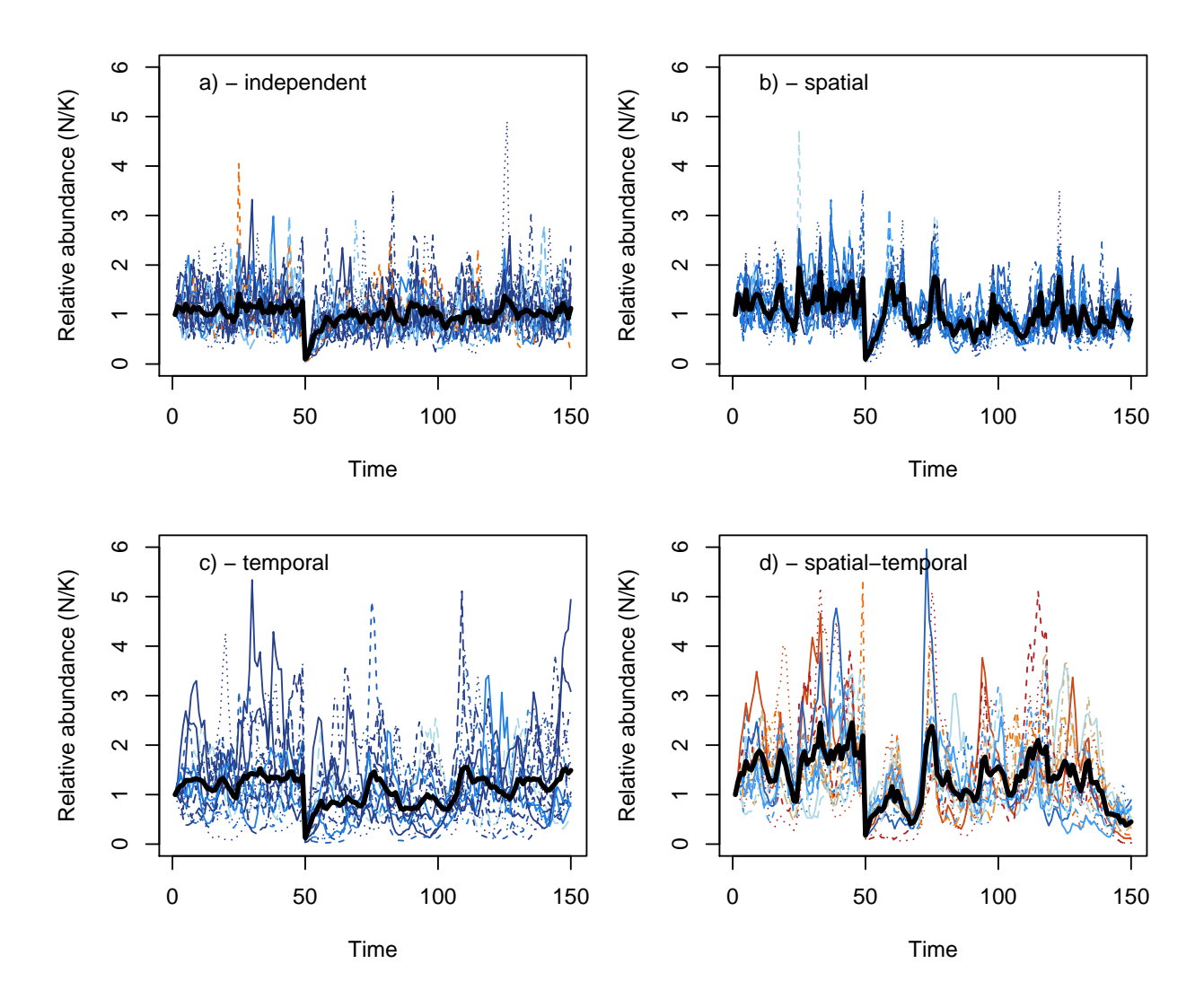


Figure S5: Metapopulation dynamics with independent (a), spatially correlated (b), temporally correlated (c), and spatio-temporally correlated (d) recruitment deviates.

113 Post-disturbance outcomes

114

115

116

117

118

119

120

We measured the following post-disturbance outcomes to track the temporal and spatial recovery regime of the metapopulation.

- 1. Recovered (a) & recovery rate (b) after disturbance:
 - a. Recovered is defined as the number of simulations where metapopulation abundance averaged 1.0 of the average pre-disturbance abundance for 5 consecutive years post-disturbance. This "recovered rate" reflects the risk of a long-term state shift in metapopulation dynamics after disturbance in the face of stochasticity.

121

122

123

125

126

128

130

131

132

133

134

135

- b. Recovery rate the number of years to average pre-disturbance abundance for 5 consecutive years. The recovery rate (either in the number of generations or in the rate of recovery per year) captures how quickly the aggregate metapopulation recovers from disturbance but doesn't take into account whether any given local patches recover to their pre-disturbance capacity.
- 2. Patch occupancy the mean number of patches with >0.1 local carrying capacity after disturbance in the short-term (5 years), medium-term (10 years), and long-term (25 years). This value characterizes the expected risk of spatial contractions or local patch collapses, and reflects how interactions between spatial structure, disturbance, and dispersal shape source-sink dynamics and the ability to provide (or not) rescue effects and recover local patches.
- 3. The ratio of expected maximum surplus production (we term MSY) to true maximum surplus production summed across all patches from fitted stock-recruitment model to aggregate across metapopulation such that:

$$\Delta_{MSY} = \frac{M\hat{S}Y_M}{\sum_{i=1}^{N_p} MSY_i} \tag{10}$$

A value of 1.0 would indicate that the disturbed metapopulation can sustain itself against the same disturbance regime as the sum of each patch independently. In other words, is the metapopulation more than $(\Delta_{MSY}>1.0)$, less than $(\Delta_{MSY}<1.0)$, or equal to the sum of its parts $(\Delta_{MSY}=1.0)$.

136 Monitoring & management at aggregate-scale

137 While true metapopulation dynamics are controlled by local patch dynamics and dispersal such that:

$$N_{it} = R_{it}\epsilon_{it} + I_{it} - D_{it} - E_{it} \tag{11}$$

$$R_{it} = \frac{\alpha_i N_{it-1}}{1 + \frac{\alpha_i - 1}{\beta_i} N_{it-1}}$$
(12)

$$MN_t = \sum_{i=1}^{N_p} N_{it} \tag{13}$$

$$MR_t = \sum_{i=1}^{N_p} R_{it} \tag{14}$$

Natural resoure managers often monitors and manages at the scale of the metapopulation. Hence, management at this scale inherently defines the stock-recruitment dynamics of the aggregate complex of patches (i.e., metapopulation) as:

$$MR_{t} = \frac{\hat{\alpha_{t}}MN_{t-1}}{1 + \frac{\hat{\alpha_{t}} - 1}{\hat{\beta_{t}}}MN_{it-1}}$$
(15)

where $\hat{\alpha}_t$ is the estimated compensation ratio averaged across the metapopulation at time t and $\hat{\beta}_t$ is the estimated carrying capacity of the entire metapopulation. Necessarily, these estimates emerge from monitoring data collected across all patches and are sensitive to the quality of the data and how local patches perform through time. For example, temporal shifts in productivity regimes may be masked if most of the data were sampled before the regime shift. To help surmount these issues, modern resource assessments use data weighting and penalties (i.e., priors) when fitting models to data.

In our assessment, we weighted recent years of sampling over more distant years such that:

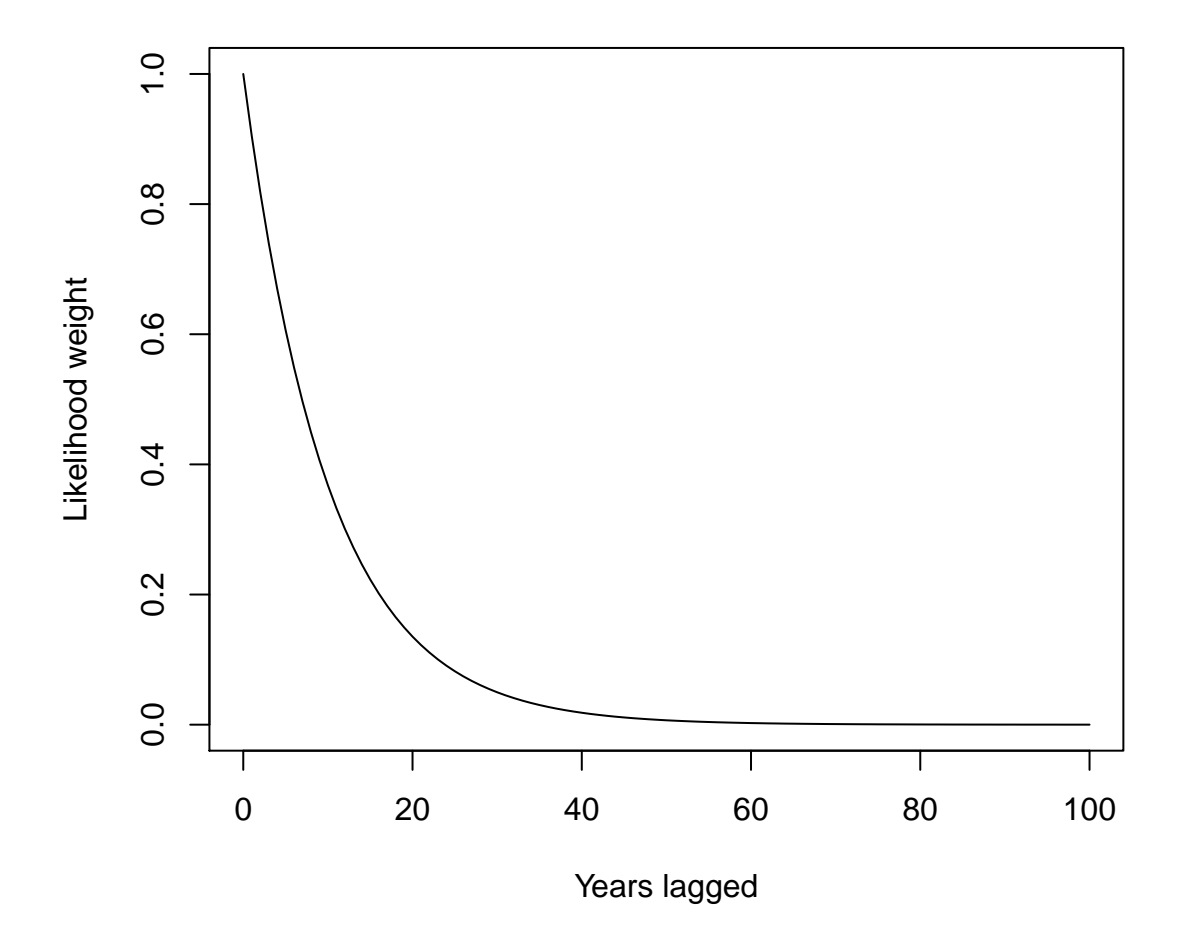


Figure S6: Likelihood weighting for samples collected over time from current year of sampling.

This forward-weighting approach increased the sensitivity of the monitoring sub-model to detect demographic changes in the post-disturbance recovery regime. Data-weighting is increasingly being used in resource monitoring, although how weights are developed and applied to data is a case-by-case basis.

Furthermore, we used penalized normal likelihoods on both $\hat{\alpha}_t$ and $\hat{\beta}_t$ such that:

$$\hat{\alpha_t} \sim N(\mu = \hat{\alpha_{t-1}}, \sigma = 3\hat{\alpha_{t-1}}) \tag{16}$$

 $_{^{152}}$ and

$$\hat{\beta}_t \sim N(\mu = \hat{\beta}_{t-1}, \sigma = 3\hat{\beta}_{t-1}) \tag{17}$$

where $\mu = \alpha_{t-1}^{-}$ and $\mu = \beta_{t-1}^{-}$ represents the best estimates from the previous assessment and the 3 in the σ term represents a 300% coefficient of variation. We used these penalized likelihoods to fit the above aggregate stock-recruitment model with lognormal error to the metapopulation stock-recruit data collected at time t. We used the following function and fitted to the below θ parameters (termed theta in the function optim() using the L-BFGS-B optimizer with a lower bound on $\hat{\alpha}$ of 1.01 (i.e., constrained to be at least above replacement).

```
SRfn <- function(theta, data, lastYr) {
    a.hat <- theta[1]
    b.hat <- exp(theta[2])
    sd.hat <- exp(theta[3])
    rec.mean <- (a.hat * data$spawners)/(1 + ((a.hat - 1)/b.hat) * data$spawners)
    # negative log likelihood on recruitment parameters
    nll <- -1 * sum(dlnorm(data$recruits, meanlog = log(rec.mean), sdlog = sd.hat,
        log = TRUE) * data$weights, na.rm = TRUE)
    # penalized likelihood on estimated alpha
    penalty1 <- -dnorm(a.hat, lastYr$alphaLstYr, 4 * lastYr$alphaLstYr, log = TRUE)
    # penalized likelihood on estimated carrying capacity
    penalty2 <- -dnorm(b.hat, lastYr$metaKLstYr, 4 * lastYr$metaKLstYr, log = TRUE)
    jnll <- sum(c(nll, penalty1, penalty2), na.rm = TRUE)
    return(jnll)
}</pre>
```

This above function allows us to assess the bias in $\hat{\alpha}_t$, $\hat{\beta}_t$, and \hat{MR}_t compared to true $\bar{\alpha}$, $\bar{\beta}$, and MR_t across the metapopulation. This then allows us to see how much information management & monitoring programs are missing when they assess metapopulations at the aggregate (rather than local) scales.

162 Finding maximum sustainable yield

Resource managers measure productivity with a variety of performance reference points (Forrest et al. 2010). 163 One of the most widely used metrics, commonly called Maximum Sustainable Yield in fisheries and other 164 harvest literature (MSY), relates to the largest loss the population can sustain over an indefinite period of 165 time while maximizing its ability to replenish itself. Under density-dependent growth, individuals' growth, survival, and reproduction at low population densities are not constrained by limited resources, but overall 167 production is low because there are few individuals. At high densities, limited resources increasingly constrain 168 individual's reproductive success until the population reaches carrying capacity, and overall production drops 169 to zero because per-capita success is low. However, at some intermediate densities, both per-capita and 170 overall production is high, and population growth is at its maximum point due to the large number of 171 reproducing individuals. At this point, there is the maximum surplus of individuals produced above 172 replacement that can help to withstand disturbance or harvest regimes and contribute to future recovery, 173 either through increasing local patch densities or by emigrating neighboring patches providing "rescue effects". 174 Under Beverton-Holt or Ricker density-dependent recuitment, however, there exists no analytical solution for 175 calculating MSY. Therefore, we used numerical methods and a one dimensional root finder to iteratively 176 search for the population mortality that maximized surplus production in the metapopulation. We term this 177 mortality F_{MSY} and can use this mortality value to calculate maximum surplus production MSY, the adult 178 densities that produce MSY (termed N_{MSY}), and the recruits that result from this (termed R_{MSY}).

```
# uniroot numerical search
yieldRoot <- function(alpha, beta, Fcur, model) {</pre>
    Ucur <- 1 - exp(-Fcur)</pre>
    if (model == "Beverton-Holt") {
        # population model is R \sim (CR * S)/(1+(CR-1)/K * S): reparameterized
        # Beverton-Holt
        adults <- beta * exp(-Fcur)
        recruits <- (alpha * adults)/(1 + ((alpha - 1)/beta) * adults)
        yield <- recruits - adults
    }
    if (model == "Ricker") {
        # population model is R ~ CR * S * e(-log(CR)/K * S): reparameterized Ricker
        adults <- beta * exp(-Fcur)
        recruits <- alpha * adults * exp((-log(alpha)/beta) * adults)
        yield <- recruits - adults
    }
    return(list(recruits = recruits, adults = adults, yield = yield))
}
# Return approximate gradient for integral
fun_yield <- function(Fcur, alpha, beta, delta, model) {</pre>
    y1 <- yieldRoot(alpha = alpha, beta = beta, Fcur = Fcur - delta/2, model = model)$yield
    y2 <- yieldRoot(alpha = alpha, beta = beta, Fcur = Fcur + delta/2, model = model)$yield
    approx.gradient <- (y2 - y1)/delta
    return(approx.gradient)
}
# uniroot search for optimal yield and Fmsy
findMSY <- function(alpha, beta, Npatches, model) {</pre>
    F_msy <- NULL
    for (i in 1:Npatches) {
        a_p <- alpha[i]</pre>
        b_p <- beta[i]</pre>
        F_msy[i] <- uniroot(fun_yield, interval = c(0, 1), extendInt = "yes",
            alpha = a_p, beta = b_p, delta = 1e-04, model = model) root
    }
    MSY <- sapply(1:Npatches, function(x) {
        yieldRoot(alpha = alpha[x], beta = beta[x], Fcur = F_msy[[x]][1], model = model)
    return(list(F_msy = F_msy, MSY = MSY))
}
```

Scenarios ■

183

184

185

We tested all combinations of the following eight processes (below) and ran a 100 bootstraps per scenario to estimate the mean for each of the above outcomes.

- 1. Homogenous and spatially variable recruitment compensation ratio across patches, i.e. intrinsic rate of population growth (α_i) .
 - 2. Homogenous and spatially variable local carrying capacity across patches, i.e. asymptote of expected recruits at high adult densities (β_i)

187

188

189

190

191

192

193

194

195

196

197

198

199

200

201

- 3. Disturbances where a proportion of individuals removed from metapopulation (e.g., 0.90) occurs.
 - a. uniform random individuals removed at equal vulnerability across all patches.
 - b. *localized*, *random* random individuals removed from randomly selected subset of patches (as long as the target individuals lost in the metapopulation can be achieved in that subset of patches)
 - c. *localized*, *extirpation* total extirpation of randomly selected subset of patches (as long as the target individuals lost in the metapopulation can be achieved in that subset of patches)
- 4. Density-independent dispersal rates ω from 0 to 20% of individuals within a patch will disperse.
- 5. Topology of the spatial networks with linear, dendritic, star, and complex networks. Each network with N_p of 16 and distance between patches \bar{d} of 1.
- 6. Stochastic recruitment deviates from low, medium, high coefficient of variation on lognormal error. Generate stochasticity in time-dynamics via random recruitement deviates away from expected.
- 7. Temporal correlation in recruitment deviates from low, medium, high correlation (i.e., good year at time t begets good year at time t+1).
 - 8. Spatial correlation in recruitment deviates among patches from low, medium, to high correlation (i.e., neighboring patches go up or down together).

202 Example results

We demonstrate our metapopulation model with an example outcome for a linear network composed of 16 patches, a dispersal rate of 0.01 and a high enough dispersal cost such that individuals are only willing to move to their closest neighboring patches. This limits the strength of potential rescue effects. For this example, patches varied in their productivity and carrying capacity but will have deterministic population dynamics.

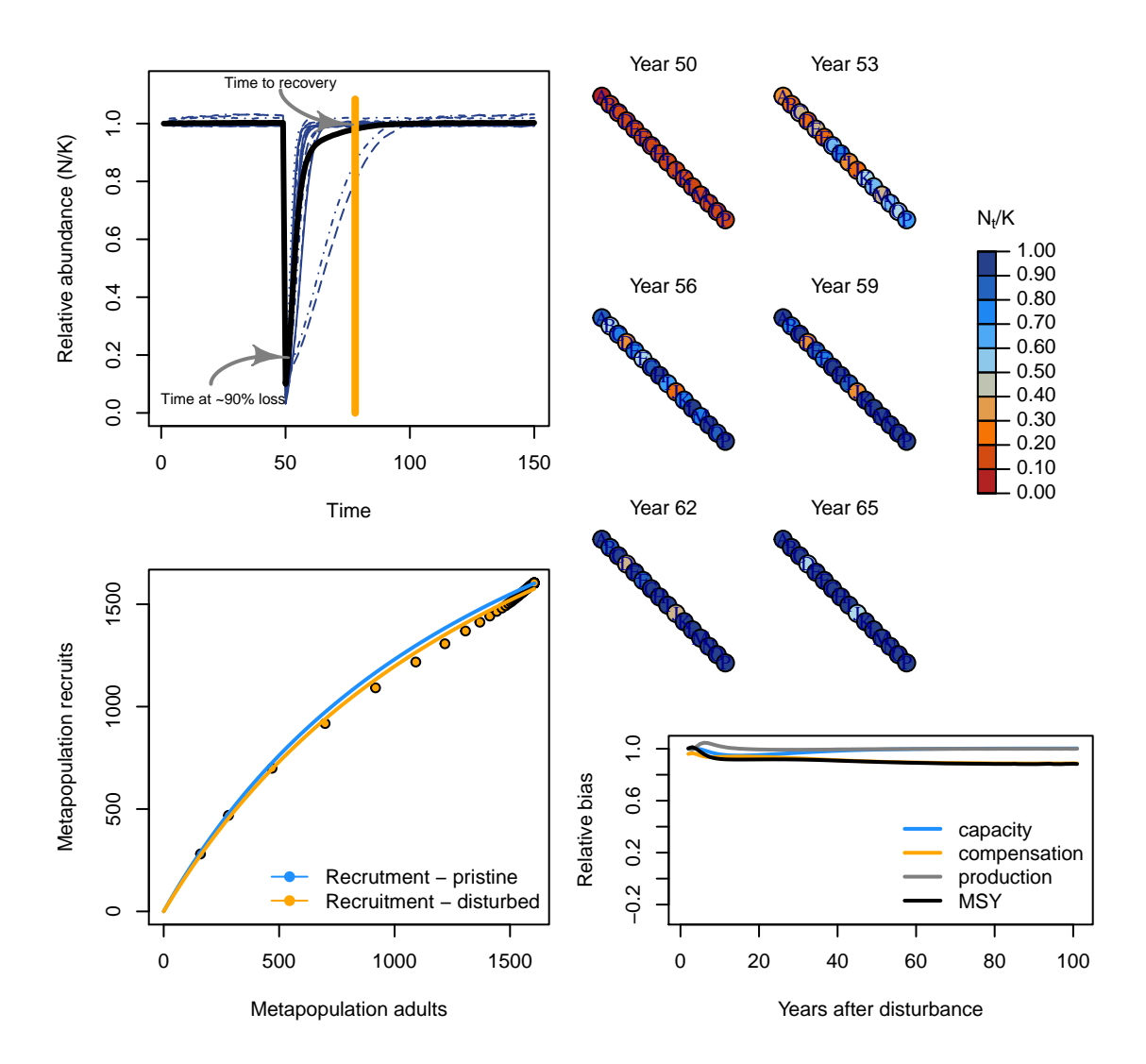


Figure S7: Spatial recovery regime of metapopulation with linear topology through time (top left) and space (top right). Recruitment dynamics before and 10 years after disturbance (bottom left). Relative bias in aggregate-scale estimates of carrying capacity, compensation ratio, and recruitment production in recovery phase (bottom right).

We can then contrast this with a different network shape, like a dendritic network.

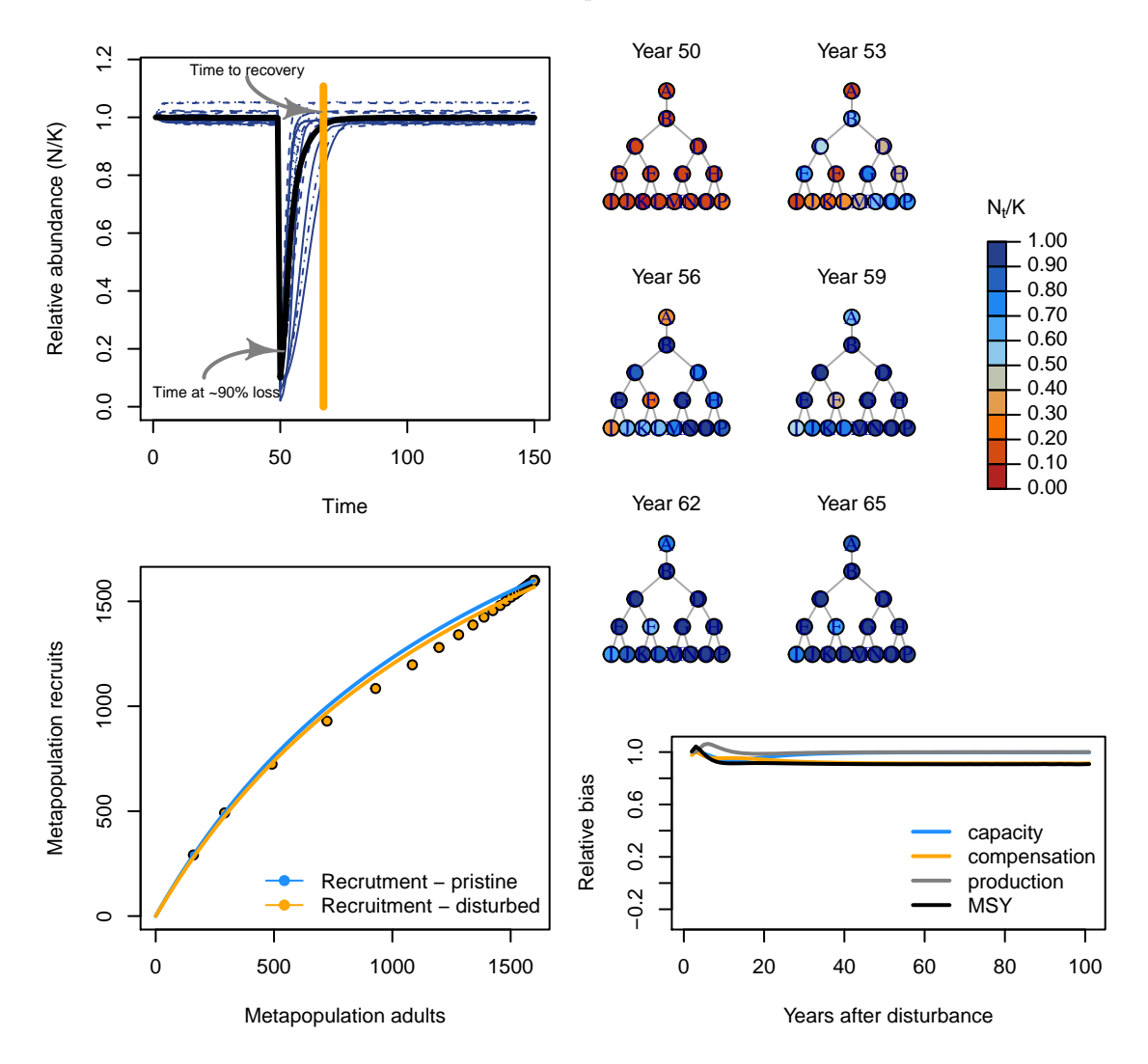


Figure S8: Spatial recovery regime of metapopulation with dendritic topology.

Now, let's add some stochasticity to recruitment and see how this affects the recovery regime.

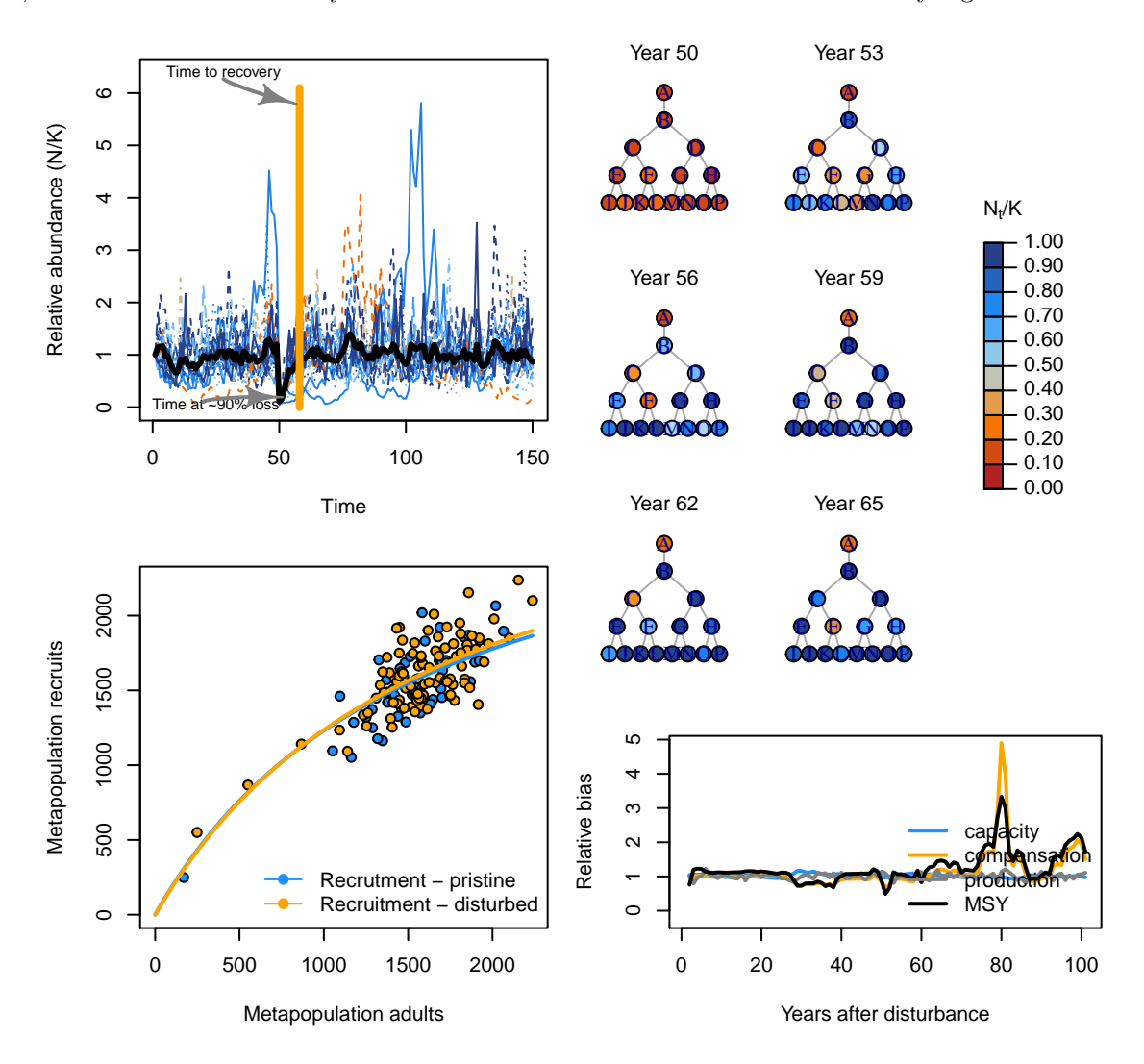


Figure S9: Spatial recovery regime of stochastic metapopulation.

Next, we can contrast with a disturbance regime where the disturbance is concentrated on local patches that can be completely extirpated (rather than the disturbance being applied proportionally across all patches e.g., a mixed-stock fishery).

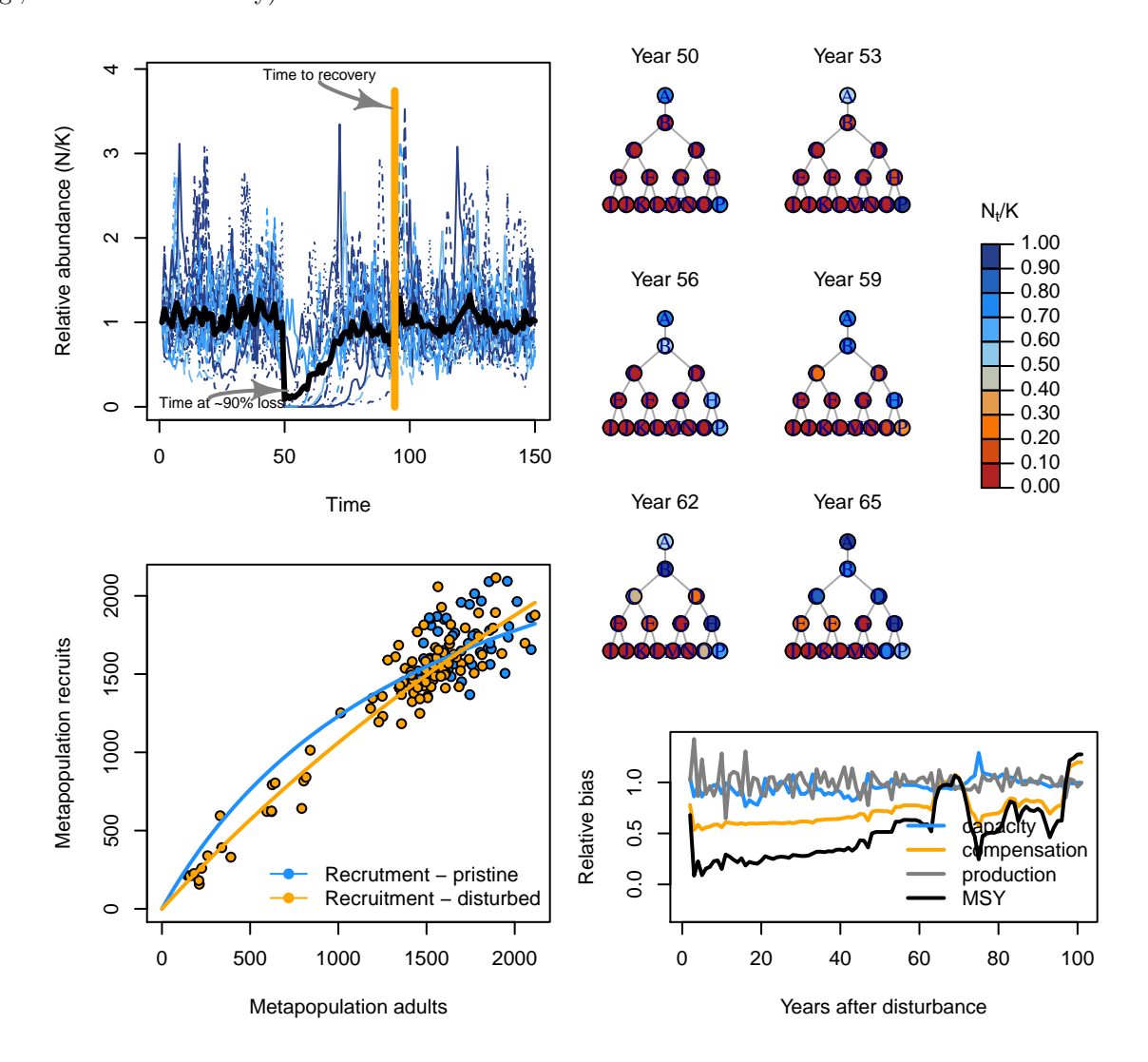


Figure S10: Spatial recovery regime of stochastic metapopulation.

General patterns

Effects of disturbance regime 214

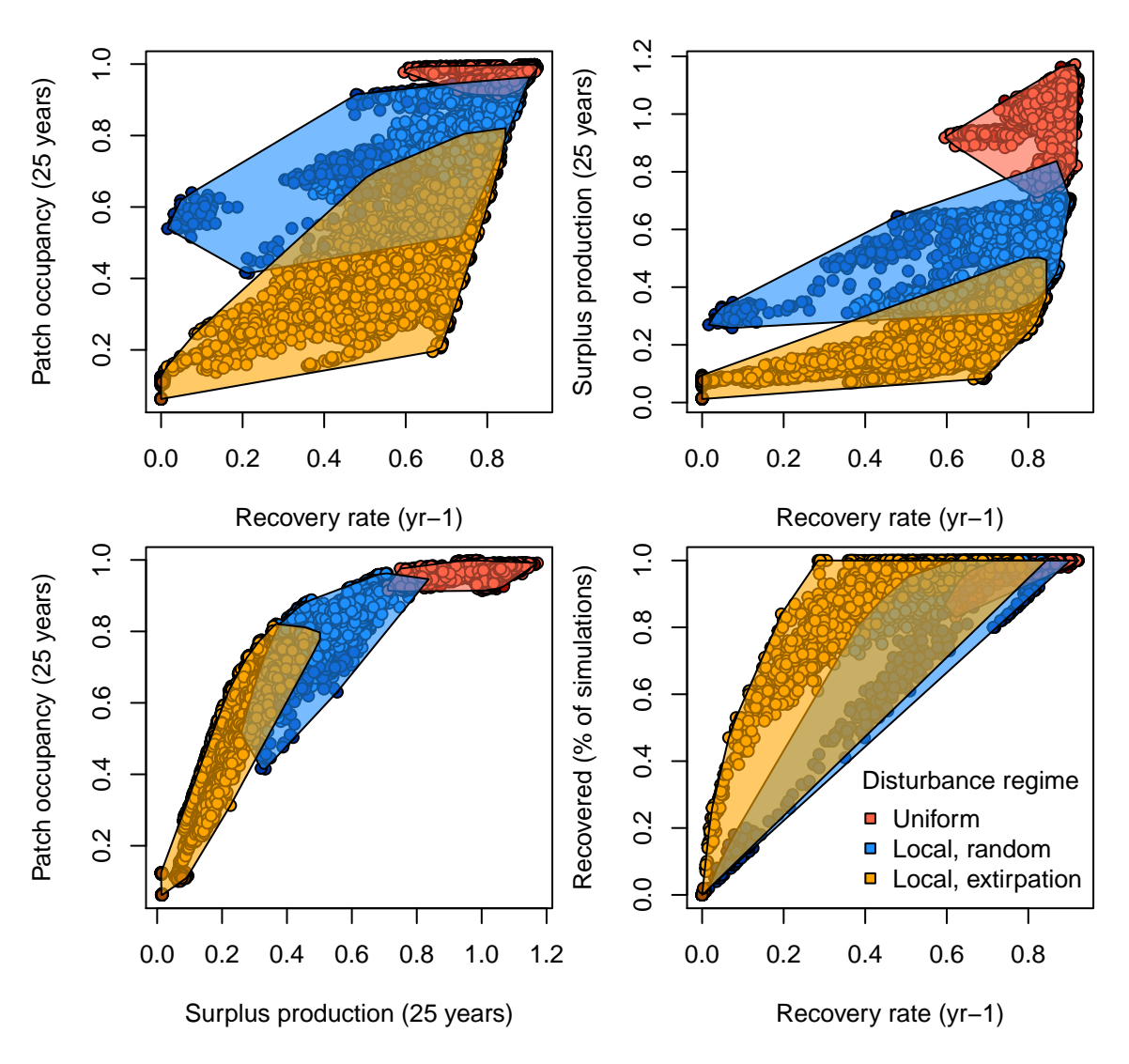


Figure S11: Spatial and temporal recovery patterns along disturbance regimes.

Role of network structure & dispersal 215

217

We now show some general patterns in how variable patch demographic rates, network structure, dispersal, 216 disturbance, recruitment stochasticity, and spatio-temporal correlations variation affects metapopulation recovery rates, maximum sustainable yield (analogous to the maximum rate of loss the system can sustain), and recovered (i.e., the number of simulations where the metapopulation fails to recover), and patch 219 occupancy (i.e., number of patches with local abundance above some baseline).

First, lets show recovery rates for a scenario where (1) patches have the same local productivities and 221 carrying capacities, (2) patches have different productivities and carrying capacities, (3) recruitment is 222 deterministic and patches are different, and (4) spatial-temporal correlation in stochastic recruitment. 223

Below, we can see three main effects on recovery rates (number of generations to reach recovery). First, 224 recovery gets faster with increased dispersal. Most of the action here takes place at low rates of dispersal 226

227

228

indicating most spatial topologies don't need much dispersal to quicken their recovery. In preliminary runs, dispersal rates of 0.05-0.2 provided similar recovery patterns. Second, more localized disturbances regimes lead to slower recovery. Third, linearized networks have slower recovery times than interconnected, complex networks suggesting that rescue effects take some time to cascade through the entire network of patches.

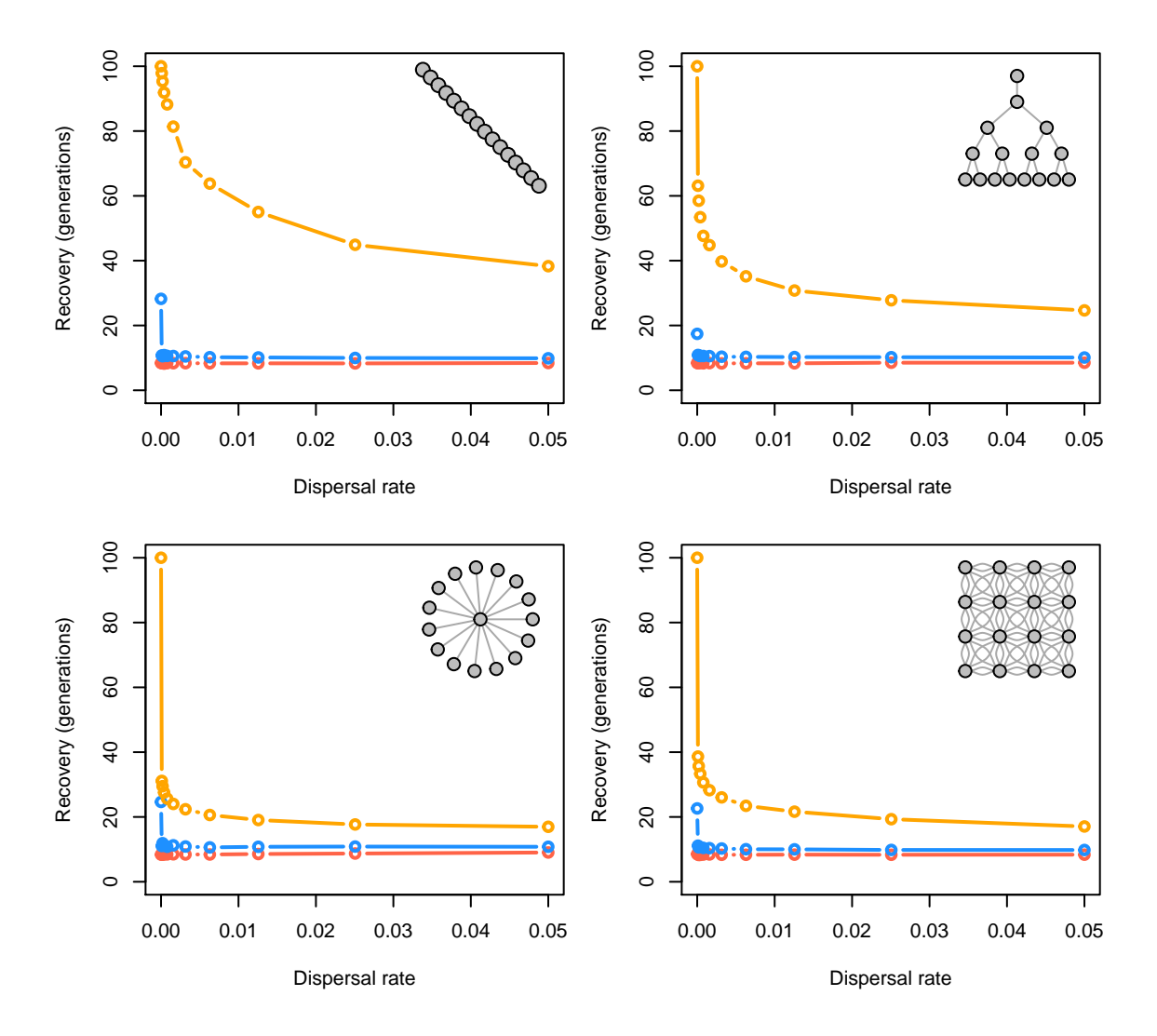


Figure S12: Recovery rates along dispersal, disturbance (red - uniform; blue - localized, random; orange - localized, extirpation), and network gradients without stochasticity.

Now, lets show recovery rates for the same scenario with deterministic recruitment but allowing for patches to vary in productivity and carrying capacity. In addition to the same three main effects of dispersal, network, and disturbance noted above, we also see variable patch productivities slows recovery across all scenarios.

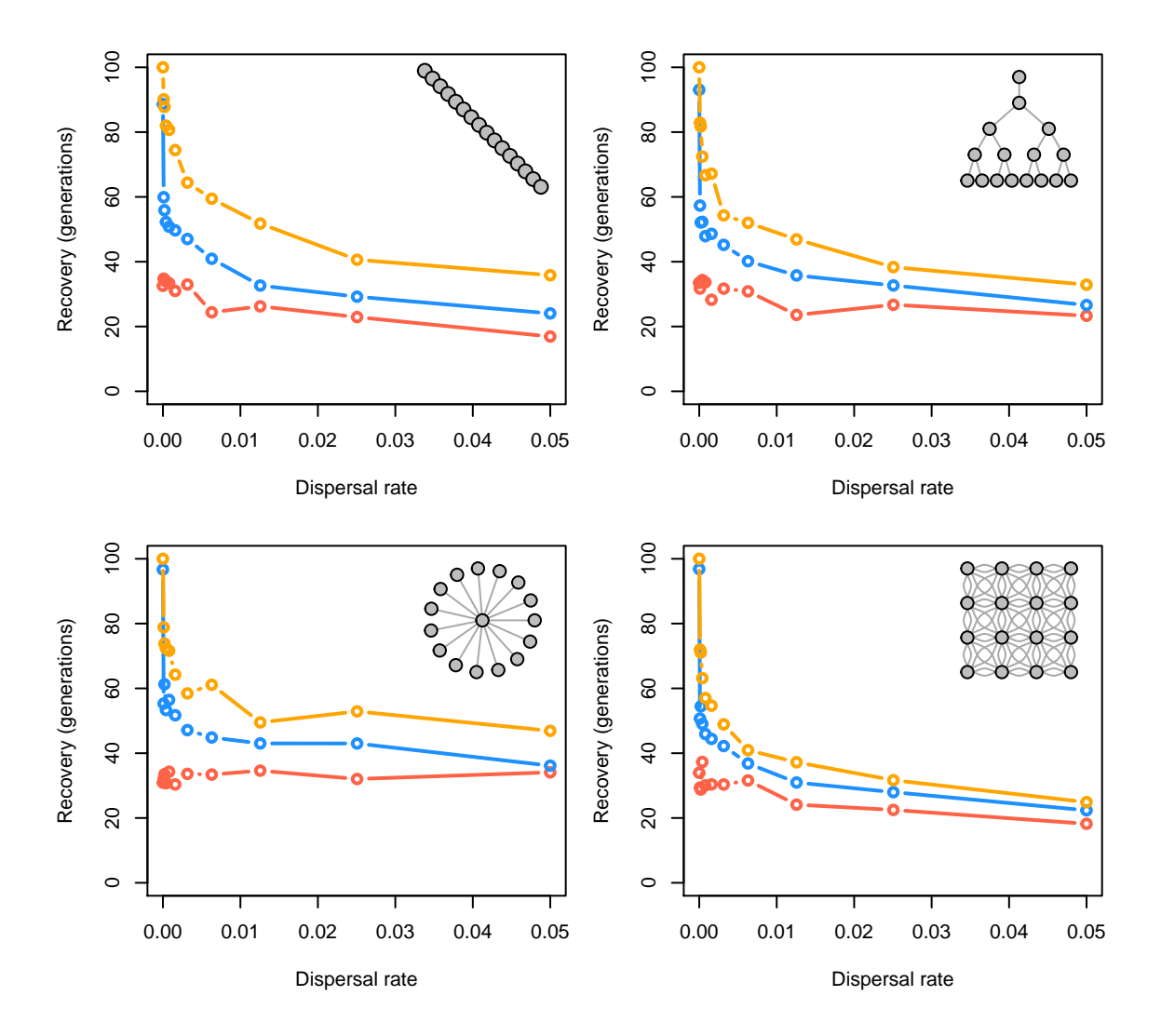


Figure S13: Recovery rates along dispersal, disturbance (red - uniform; blue - localized, random; orange - localized, extirpation), and network gradients with variable local productivity and carrying capacities.

Now, lets show recovery rates for the same scenario but allowing for recruitment to be stochastic (but patches are the same in demography). We see the same three main effects of dispersal, network, and disturbance noted above. We also see a few subtle changes: (1) stochasticity slows recovery for uniform and local disturbance, but (2) quickens recovery for extreme local disturbance.

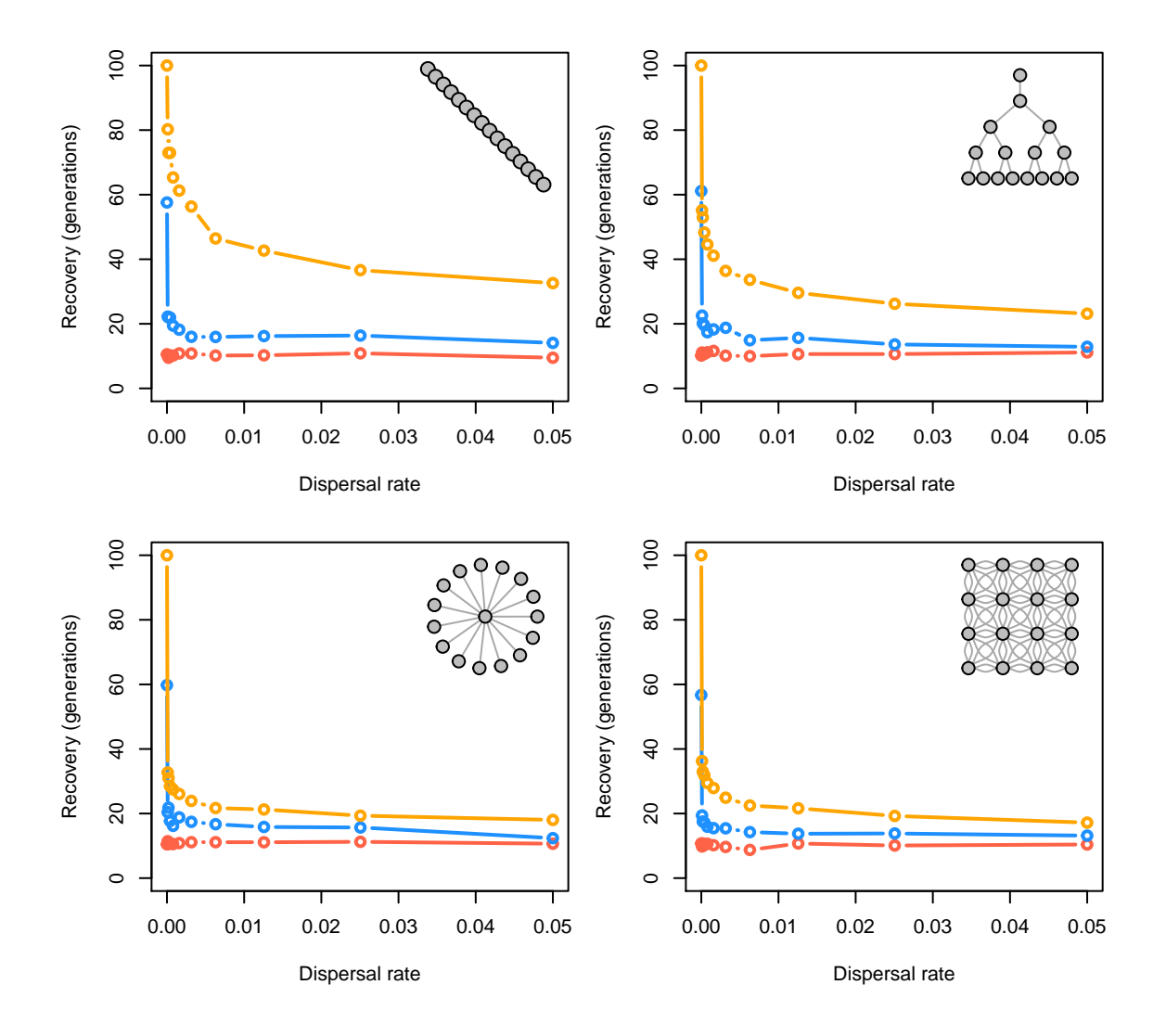


Figure S14: Recovery rates along dispersal, disturbance (red - uniform; blue - localized, random; orange - localized, extirpation), and network gradients with stochasticity.

Now, lets show recovery rates for the same scenarios but with spatial and temporal correlations in recruitment stochasticity. In addition to the same effects of stochasticity, we also generally see a small effect of slower recovery times for uniform and local disturbance, but faster recovery times for extreme localized disturbance.

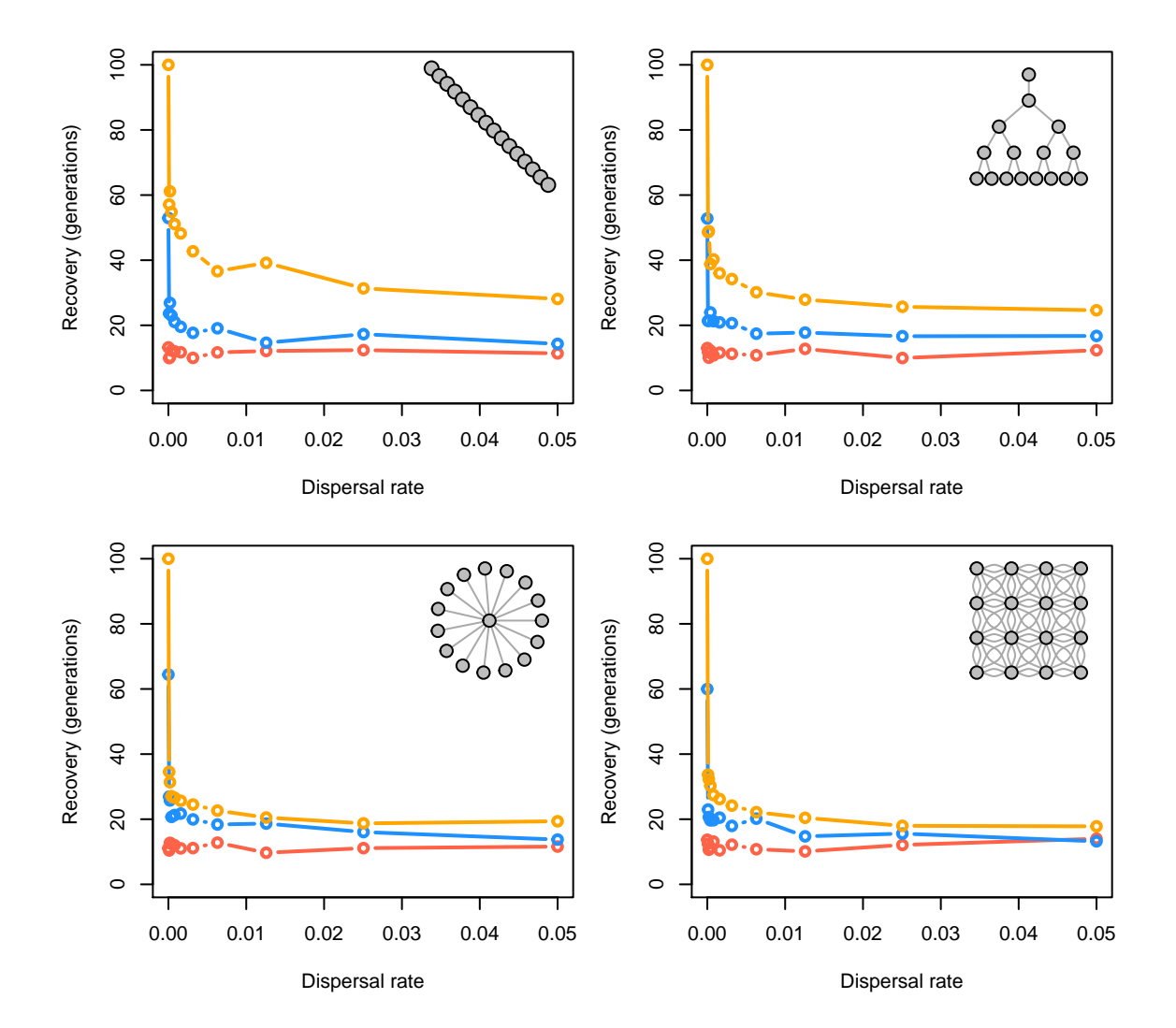


Figure S15: Recovery rates along dispersal, disturbance (red - uniform; blue - localized, random; orange - localized, extirpation), and network gradients with high spatial-temporal correlation in recruitment variation.

General patterns in MSY

MSY with deterministic recruitment where patches are the same

We now show similar patterns in how the maximum surplus production of the whole metapopulation (i.e., MSY) shifts in the first 25 years post-disturbance compared to the sum of MSY for each patch. A value of 1.0 would indicate that the disturbed metapopulation can sustain itself against the same disturbance regime as the sum of each patch independently. In other words, is the metapopulation more, less, or equal to the sum of its parts.

We will show 25-year MSY patterns for a scenario where (1) patches have the same local productivities and carrying capacities, (2) patches have different productivities and carrying capacities, (3) recruitment is deterministic and patches are different, (4) spatial-temporal correlation in stochastic recruitment.

Below, we can see three main effects on recovery rates (number of generations to reach recovery). First, recovery gets faster with increased dispersal. Most of the action here takes place at low rates of dispersal indicating most spatial topologies don't need much dispersal to quicken their recovery. In preliminary runs, dispersal rates of 0.05-0.2 provided similar recovery patterns. Second, more localized disturbances regimes lead to slower recovery. Third, linearized networks have slower recovery times than interconnected, complex networks suggesting that rescue effects take some time to cascade through the entire network of patches.

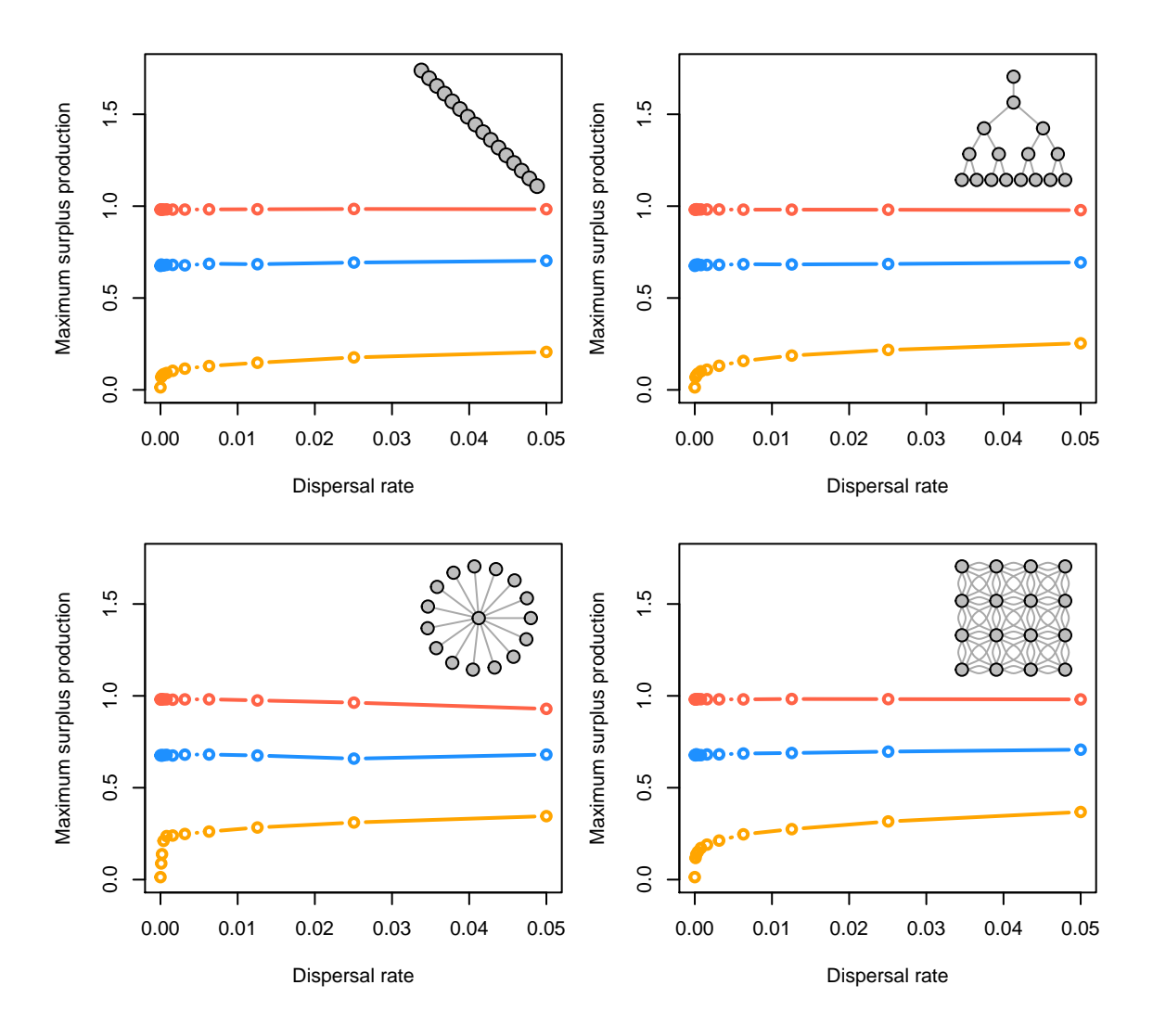


Figure S16: Maximum surplus production along dispersal, disturbance (red - uniform; blue - localized, random; orange - localized, extirpation), and network gradients with deterministic recruitment and the same patches.

256 MSY with variable patches

Now, we illustrate how variable patch demography affects the 25-year average MSY.

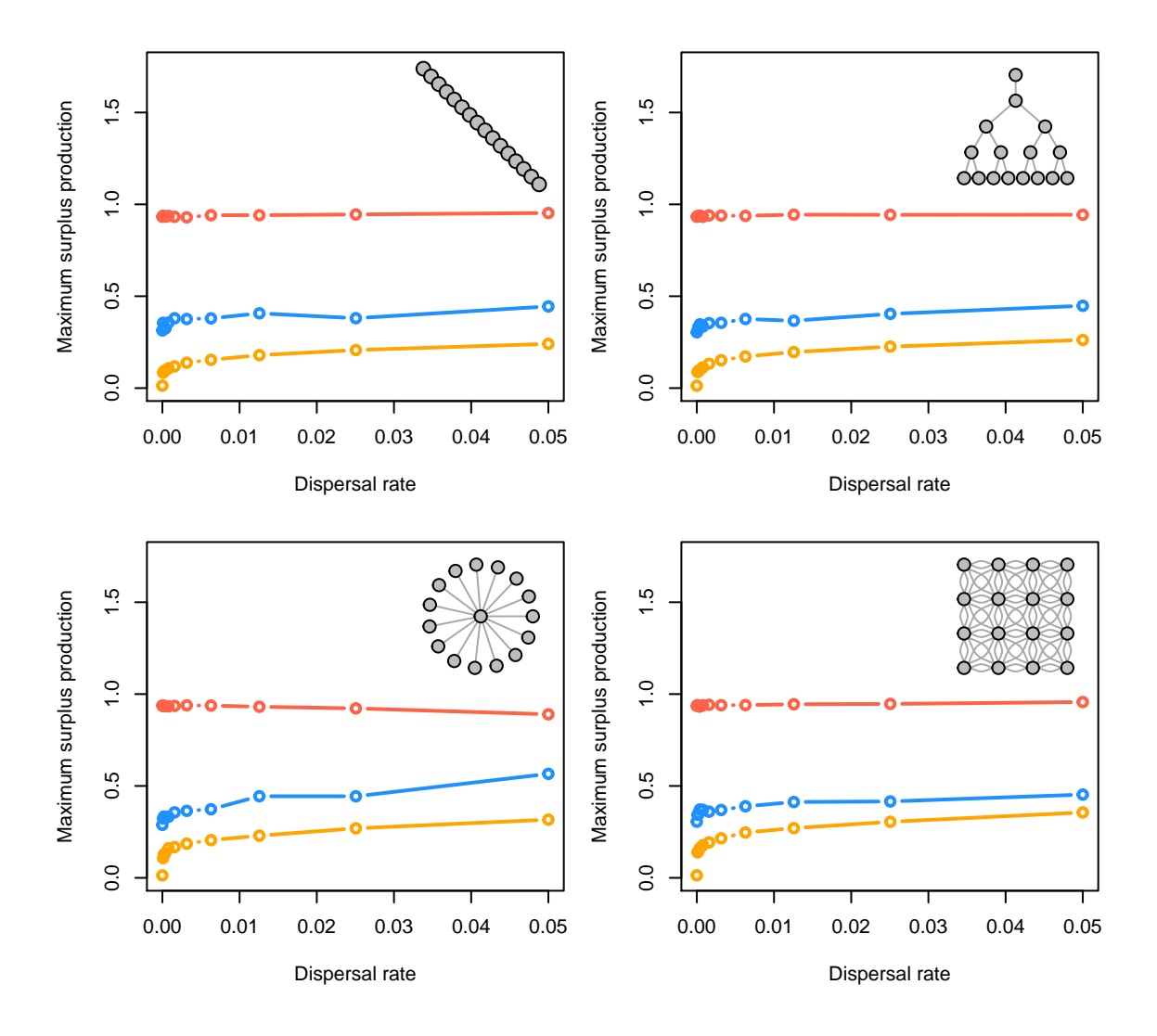


Figure S17: Maximum surplus production along dispersal, disturbance (red - uniform; blue - localized, random; orange - localized, extirpation), and network gradients with variable patches.

258 MSY with variable patches and stochasticity

Now, we illustrate how variable patch demography affects the 25-year average MSY.

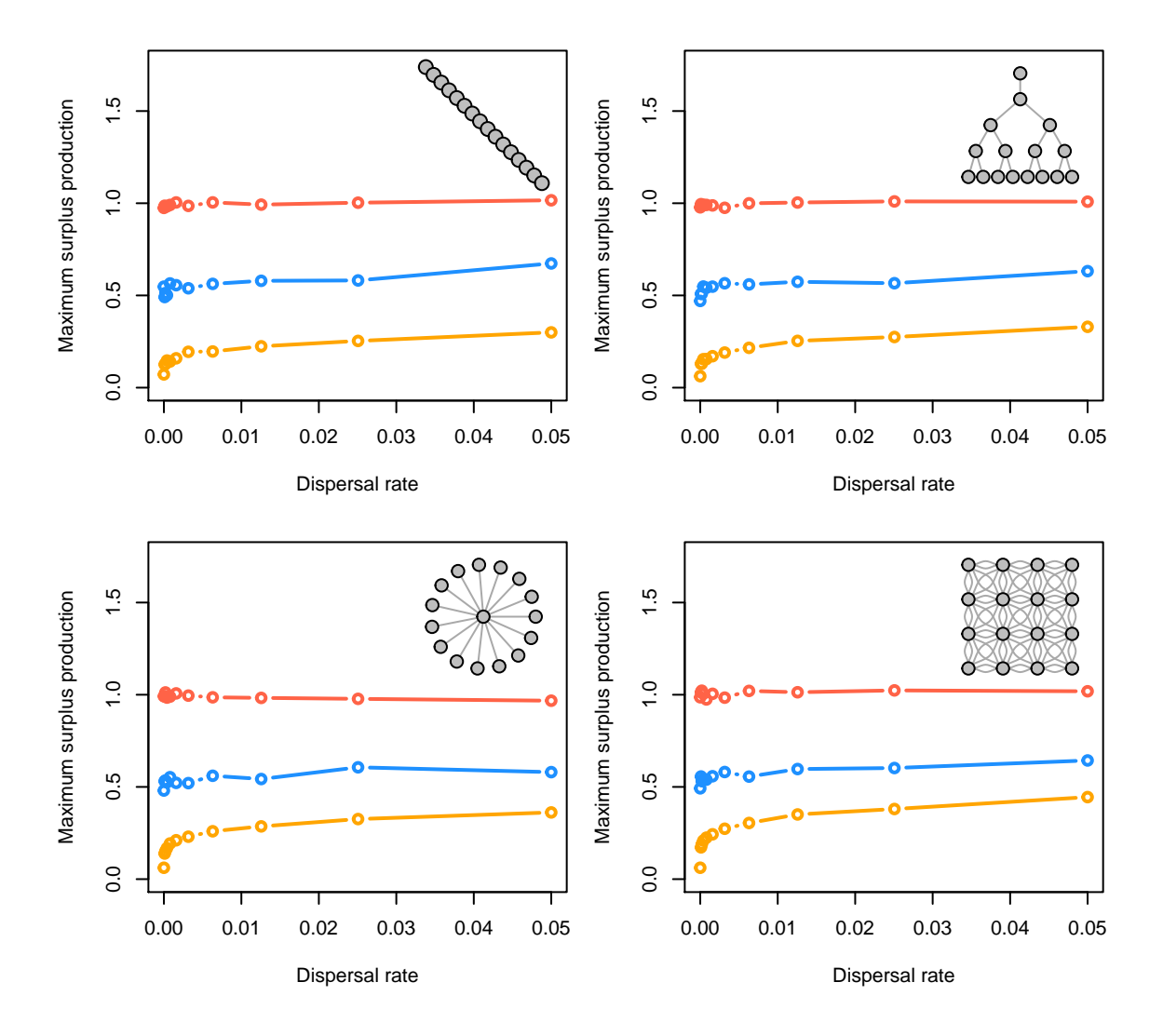


Figure S18: Maximum surplus production along dispersal, disturbance (red - uniform; blue - localized, random; orange - localized, extirpation), and network gradients with variable patches and stochasticity.

²⁶⁰ MSY with variable patches, and spatio-temporally correlated stochasticity

Now, we illustrate how variable patch demography and high spatial-temporal correlations in stochastic recruitment affects the 25-year average MSY.

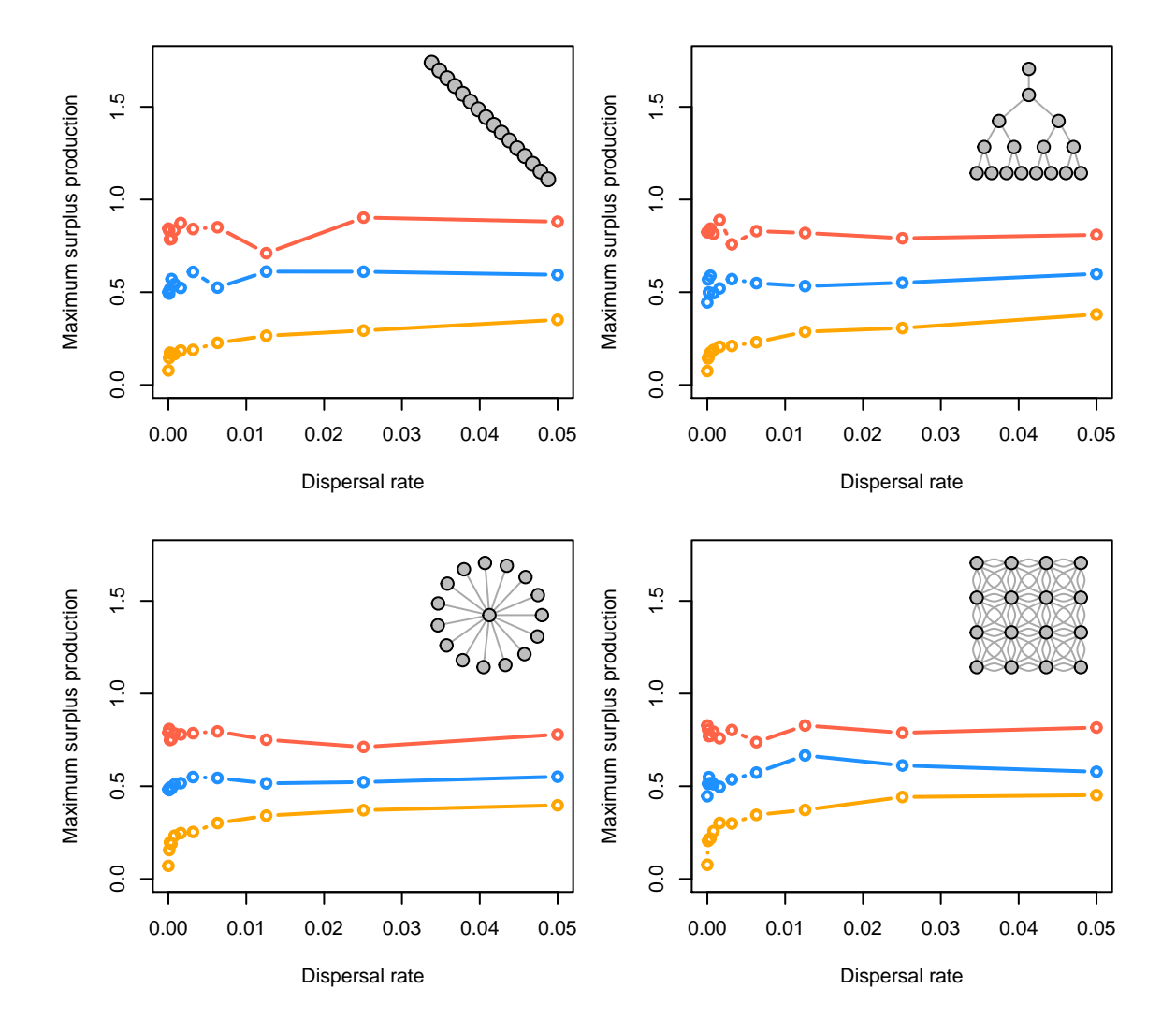


Figure S19: Maximum surplus production along dispersal, disturbance (red - uniform; blue - localized, random; orange - localized, extirpation), and network gradients with high spatial-temporal correlation in recruitment stochasticity and variable patches.

264

265

266

267

268

General patterns in the risk of hysteresis & state shifts

We now show similar patterns in the lack of recovery across the metapopulation after 100 generations post-disturbance. Recovered % is defined as the number of simulations where metapopulation abundance averaged 1.0 of the average pre-disturbance abundance for 5 consecutive years after disturbance. This "recovered rate" reflects the risk of a long-term state shift in metapopulation dynamics after disturbance in the face of stochasticity. We start with a scenario with deterministic recruitment where patches are the same.

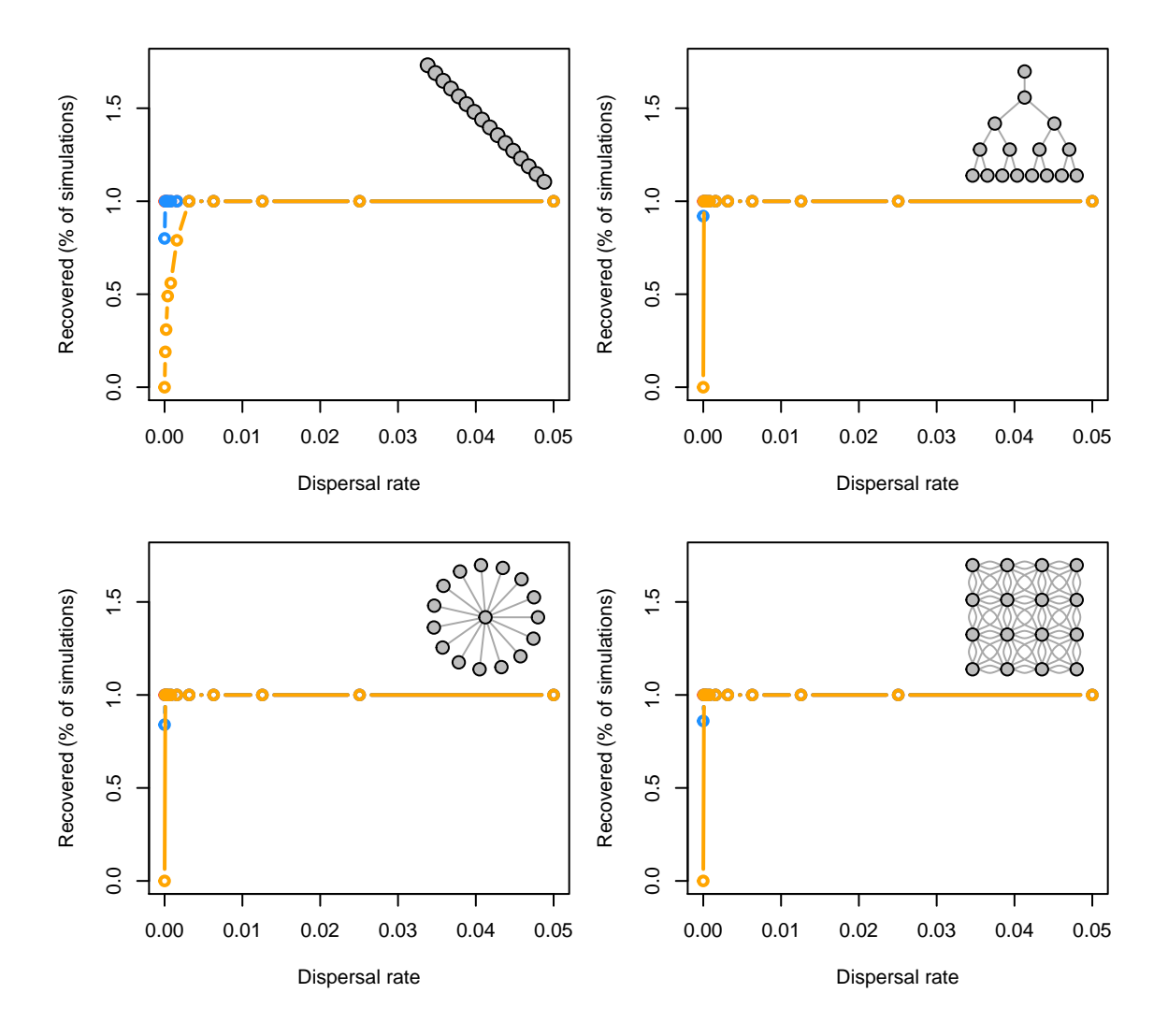


Figure S20: Risk of state shift after 100 generations along dispersal, disturbance (red - uniform; blue - localized, random; orange - localized, extirpation), and network gradients with high spatial-temporal correlation in recruitment variation.

State shifts with variable patches

Now, we illustrate how variable patch demography affects the risk of a state shift.

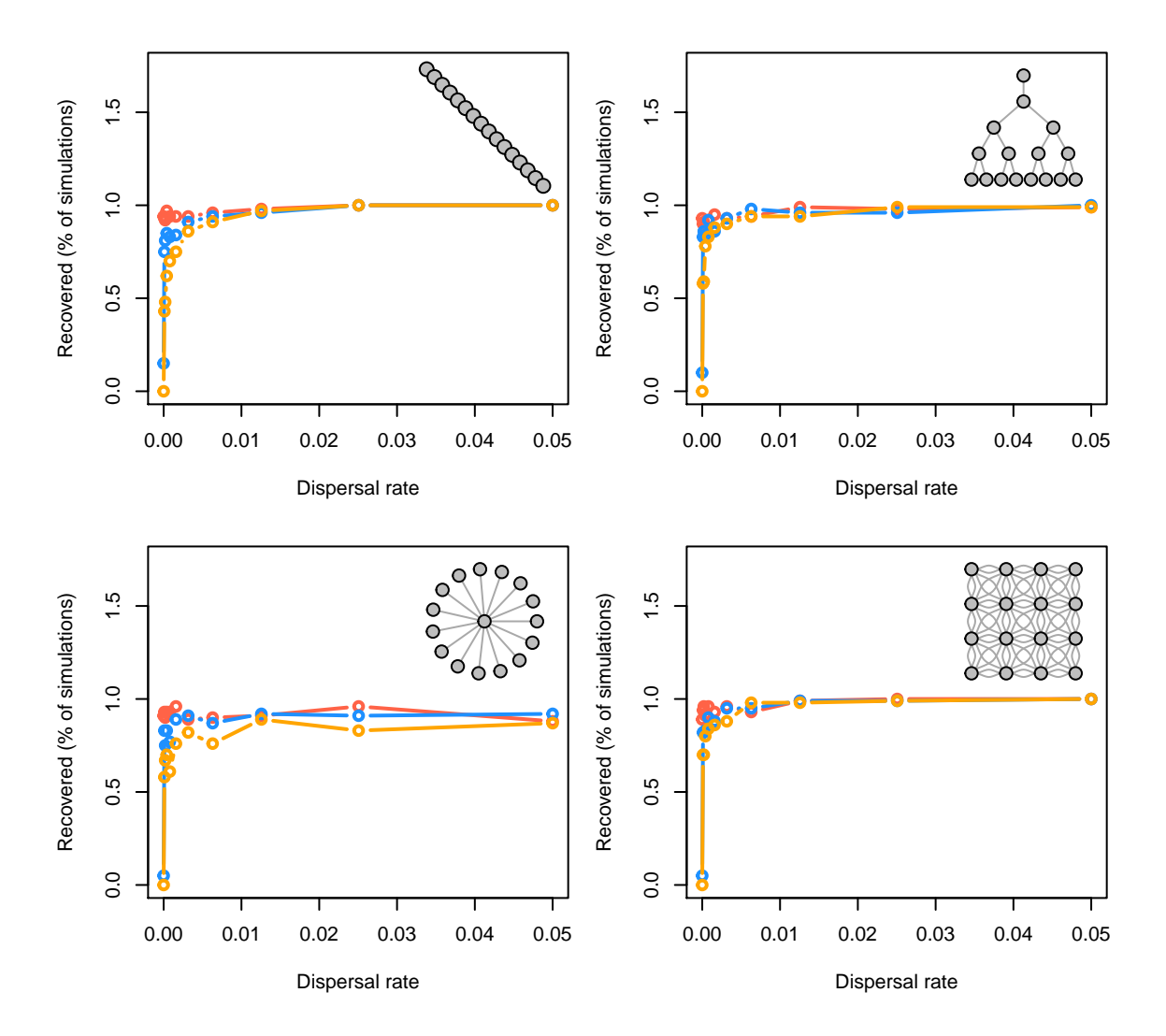


Figure S21: Risk of state shift after 100 generations along dispersal, disturbance (red - uniform; blue - localized, random; orange - localized, extirpation), and network gradients with variable patches.

State shifts with variable patches and stochasticity

Now, we illustrate how variable patch demography and stochastic recruitment affects the risk of state shift.

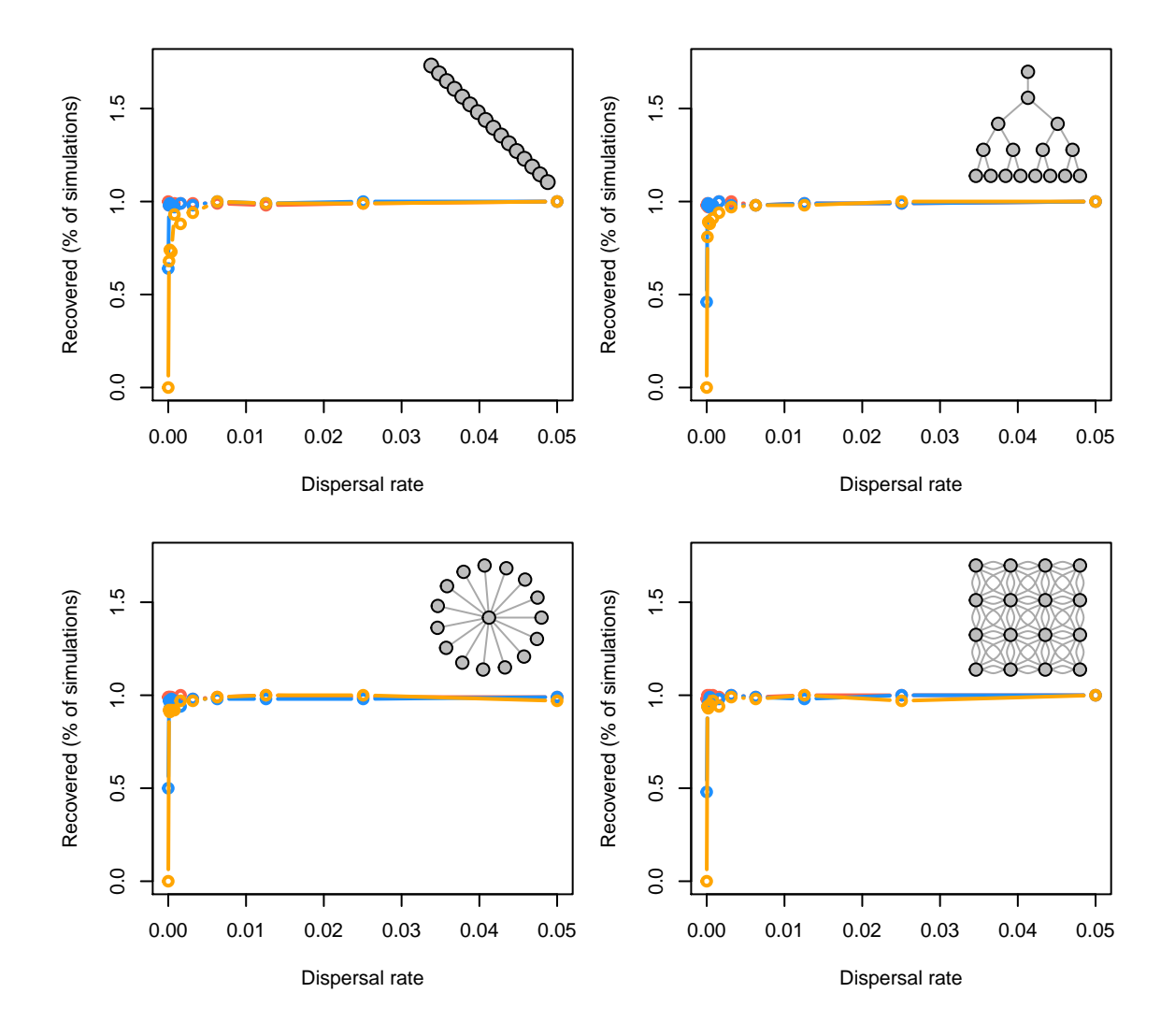


Figure S22: Risk of state shift after 100 generations along dispersal, disturbance (red - uniform; blue - localized, random; orange - localized, extirpation), and network gradients with variable patches and stochastic recruitment.

273 State shifts with variable patches, and spatio-temporally correlated stochasticity

Now, we illustrate how variable patch demography and high spatial-temporal correlations in stochastic recruitment affects the risk of a state shift.

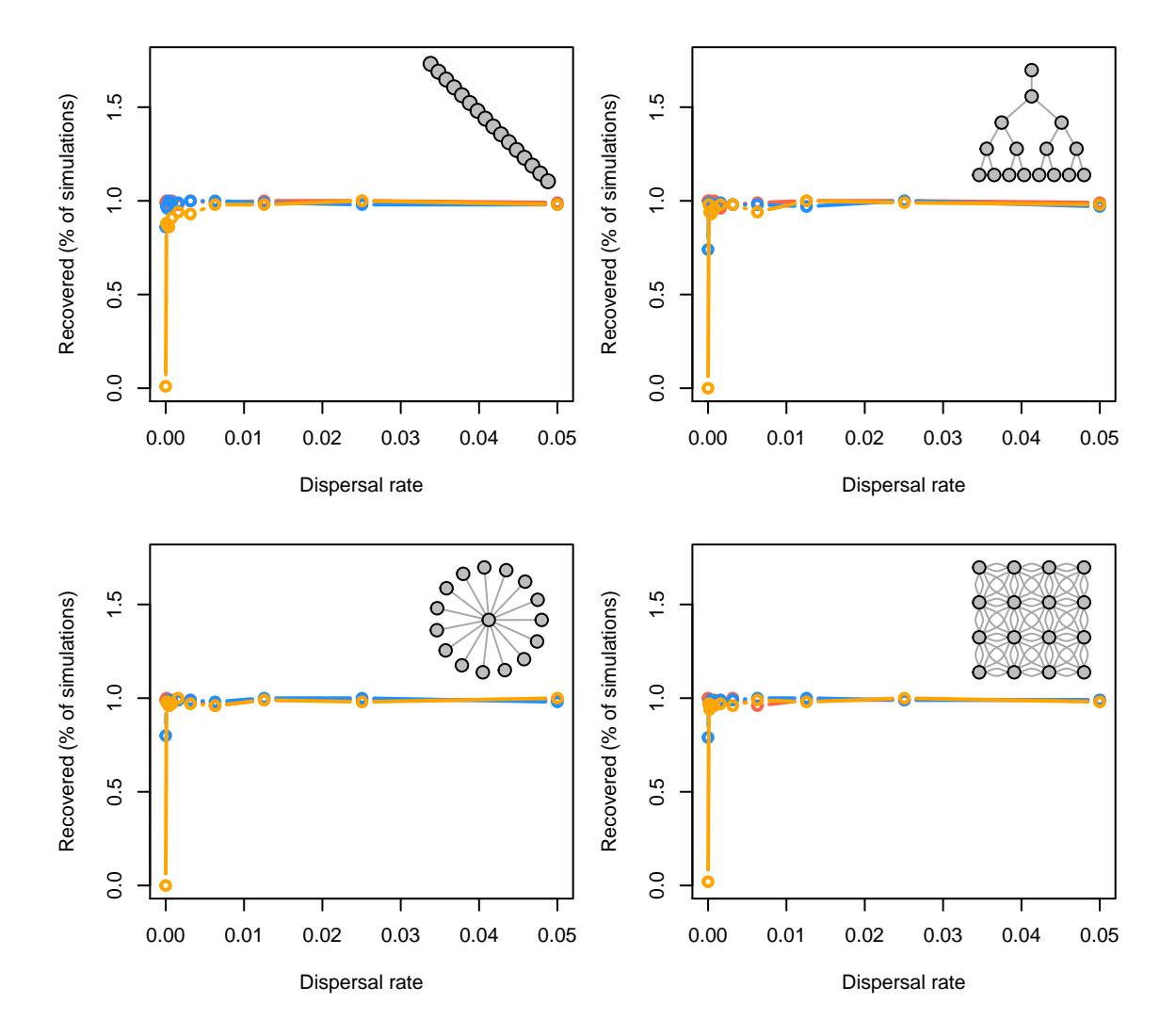


Figure S23: Risk of state shift (lack of recovery or spatial contraction) after 100 generations along dispersal, disturbance (red - uniform; blue - localized, random; orange - localized, extirpation), and network gradients with variable patches, and spatial-temporal correlations in stochastic recruitment.

277

278

279

280

281

General patterns in the risk of spatial contraction

We now show similar patterns in patch occupancy after 25 years post-disturbance. Patch occupancy is defined as the average number of patches that fail to recover above 0.1 pre-disturbance abundance for scenario with deterministic recruitment where patches are the same. Patch occupancy characterizes the expected risk of spatial contractions or local patch collapses, and reflects how interactions between spatial structure, disturbance, and dispersal affect source-sink dynamics and the provisioning of rescue effects to local patches.

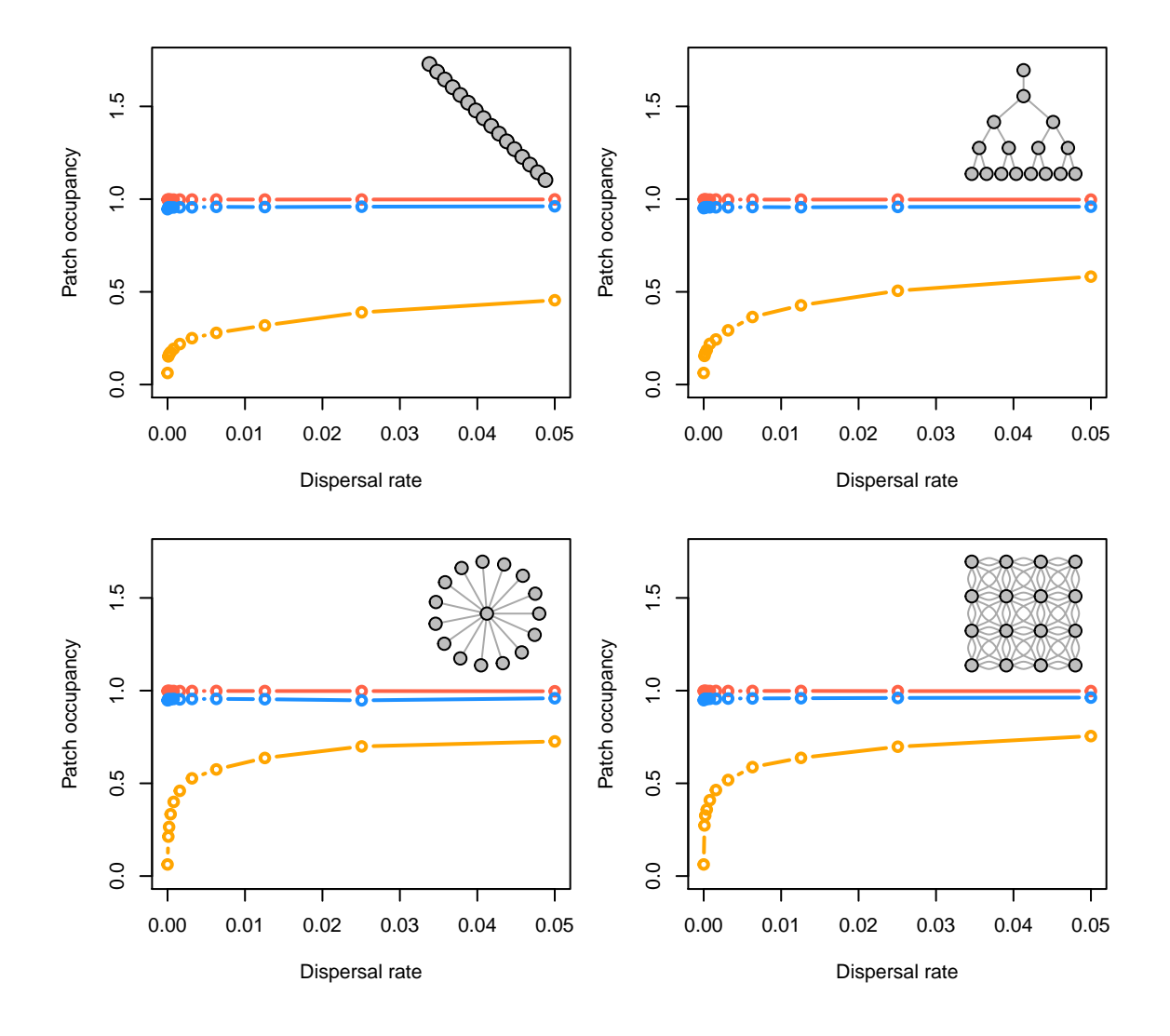


Figure S24: Patch occupancy after 25 years along dispersal, disturbance (red - uniform; blue - localized, random; orange - localized, extirpation), and network gradients with deterministic recruitment and homogeouns patches.

282 Patch occupancy with variable patches

Now, we illustrate how variable patch demography affects patch occupancy.

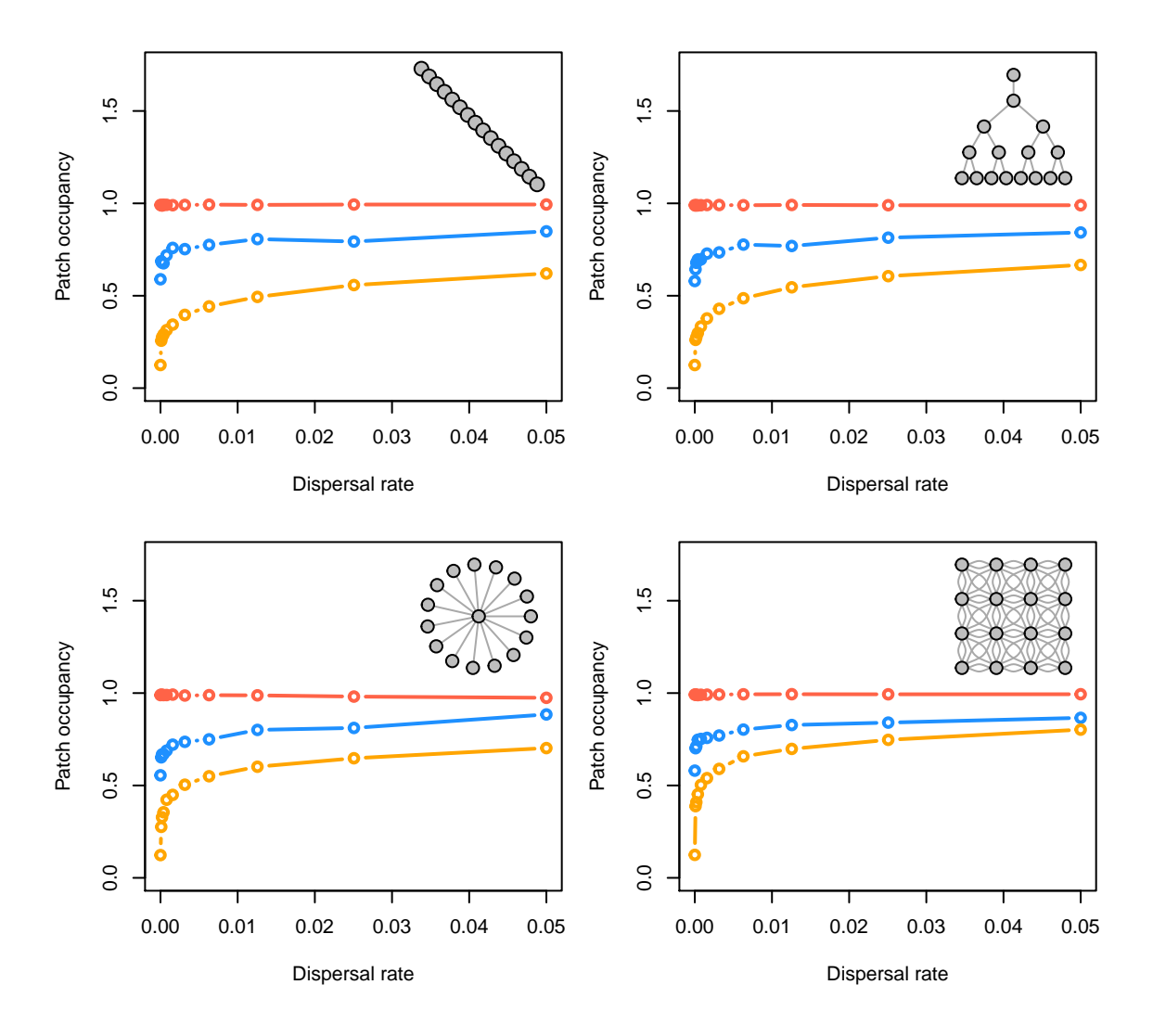


Figure S25: Patch occupancy after 25 years along dispersal, disturbance (red - uniform; blue - localized, random; orange - localized, extirpation), and network gradients with variable patches.

²⁸⁴ Patch occupancy with variable patches and stochasticity

Now, we illustrate how variable patch demography and stochastic recruitment affects long-term patch occupancy.

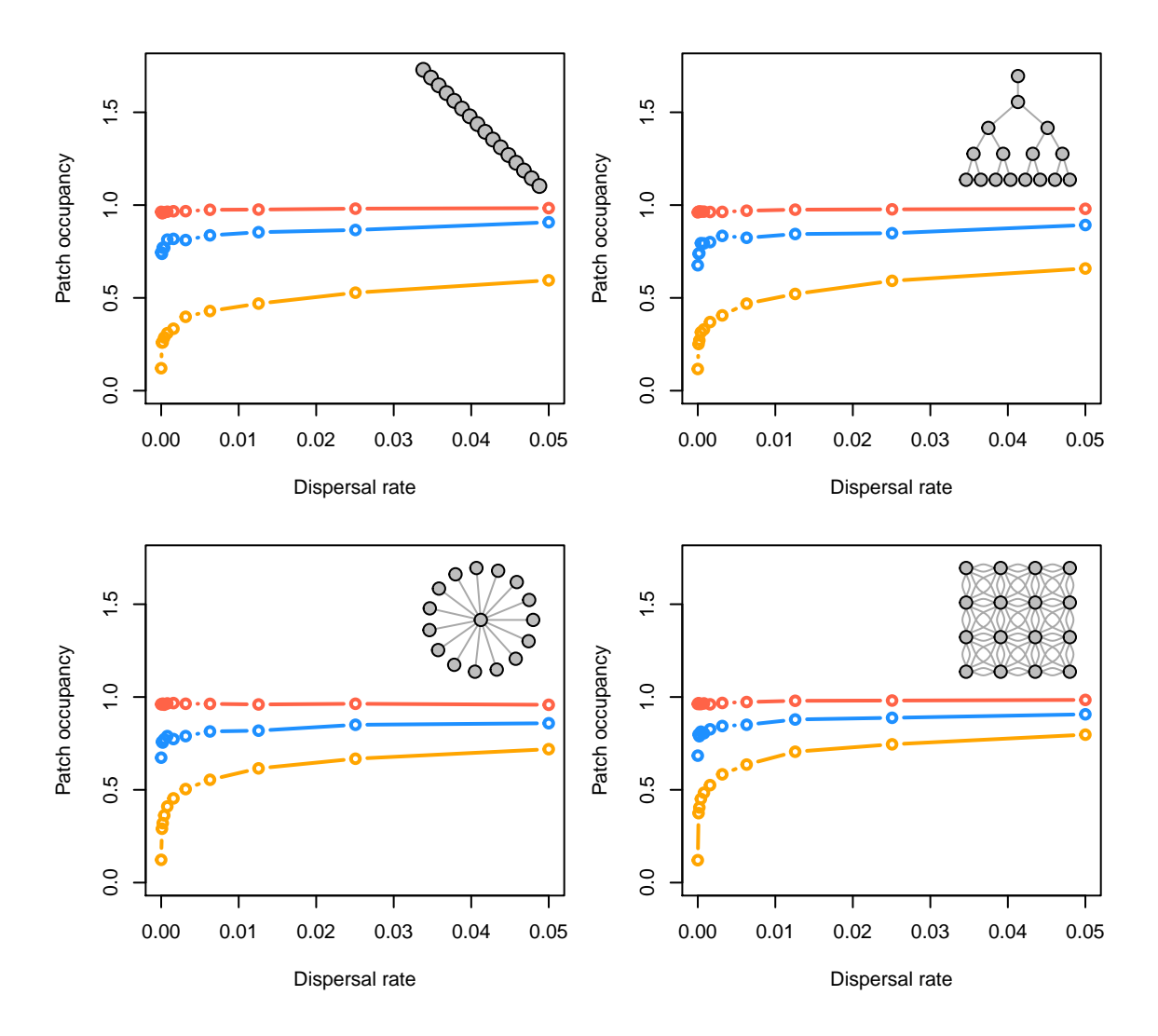


Figure S26: Patch occupancy after 25 years along dispersal, disturbance (red - uniform; blue - localized, random; orange - localized, extirpation), and network gradients with variable patches and stochastic recruitment.

- Patch occupancy with variable patches and spatio-temporally correlated stochasticity in recruitment
- Now, we illustrate how variable patch demography and high spatial-temporal correlations in stochastic recrtuitment affects long-term patch occupancy.

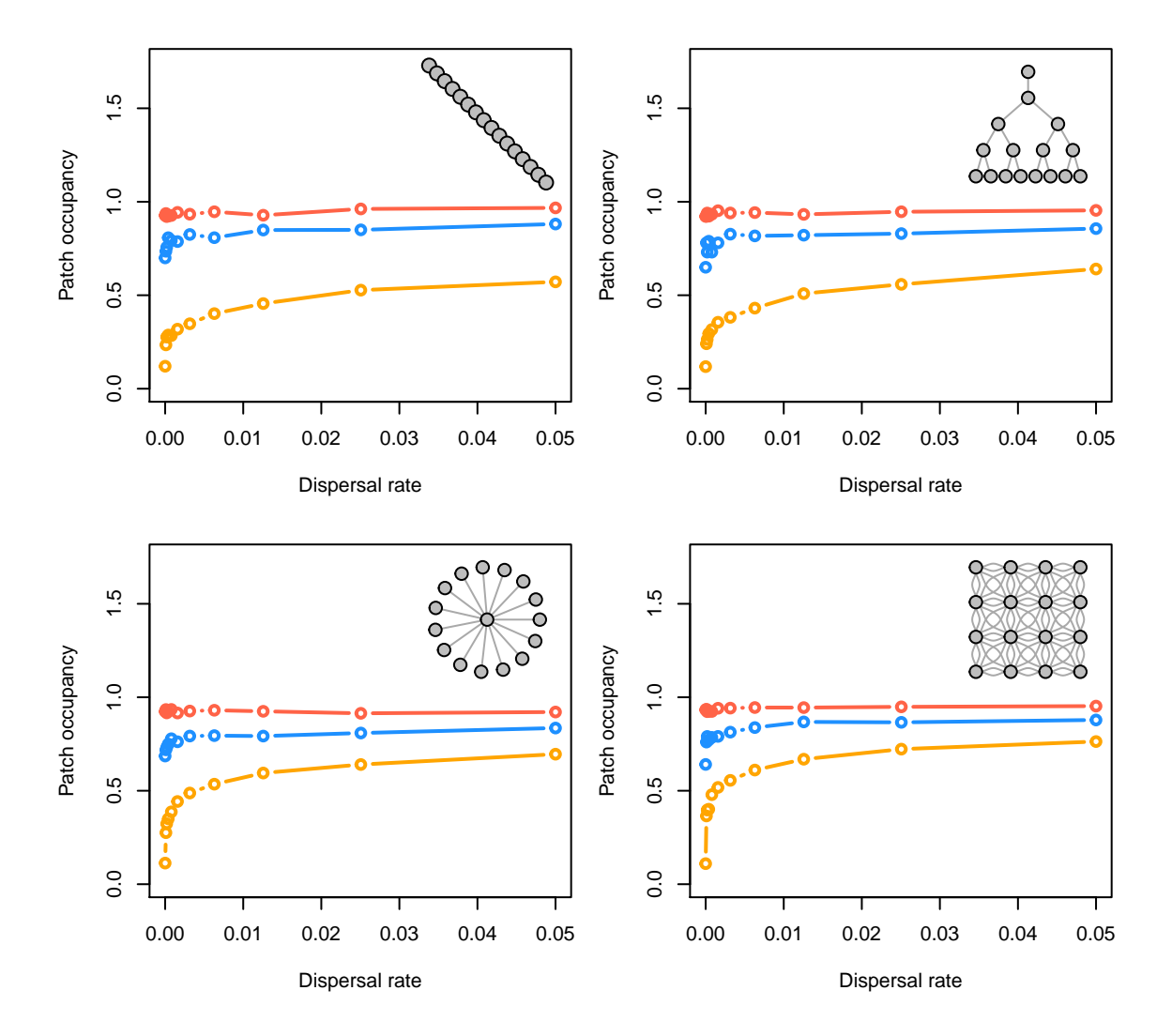


Figure S27: Patch occupancy after 25 years along dispersal, disturbance (red - uniform; blue - localized, random; orange - localized, extirpation), and network gradients with variable patches and spatial-temporal correlations in stochastic recruitment.

References

- Anderson, S.C., Moore, J.W., McClure, M.M., Dulvy, N.K. & Cooper, A.B. (2015). Portfolio conservation of
- metapopulations under climate change. Ecological Applications 25 (2), 559-572. Ecological Applications, 25,
- 294 559-572.
- ²⁹⁵ Csardi, G. & Nepusz, T. (2006). The igraph software package for complex network research. *InterJournal*,
- ²⁹⁶ Complex Systems, 1695.
- Forrest, R.E., McAllister, M.K., Dorn, M.W., Martell, S.J. & Stanley, R.D. (2010). Hierarchical Bayesian
- estimation of recruitment parameters and reference points for Pacific rockfishes (Sebastes spp.) under
- alternative assumptions about the stock-recruit function. Canadian Journal of Fisheries and Aquatic
- 300 Sciences, **67**, 1611–1634.
- Hanski, I. (1998). Metapopulation dynamics. Nature, 396, 41–49.
- ³⁰² Yeakel, J.D., Moore, J.W., Guimarães, P.R. & Aguiar, M.A. de. (2014). Synchronisation and stability in
- river metapopulation networks. Ecology Letters, 17, 273–283.